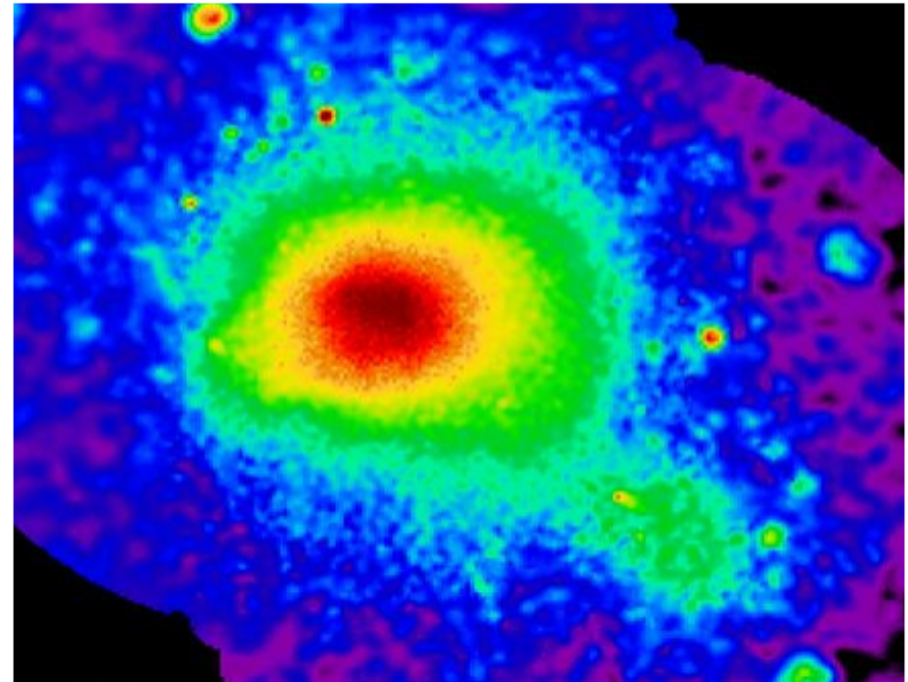
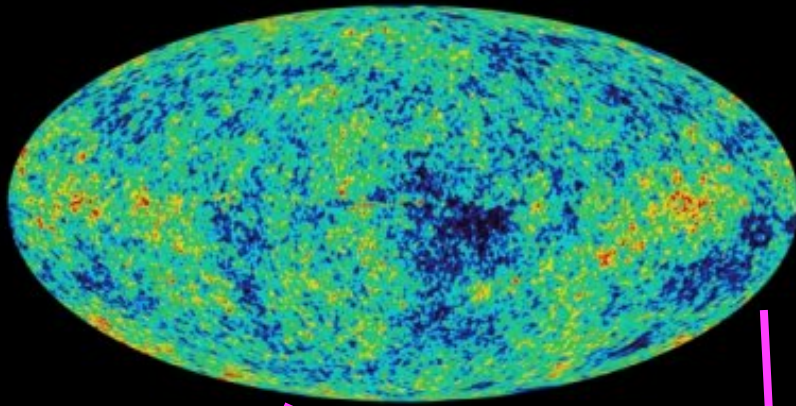


# Mass profiles and concentrations in X-ray luminous galaxy clusters



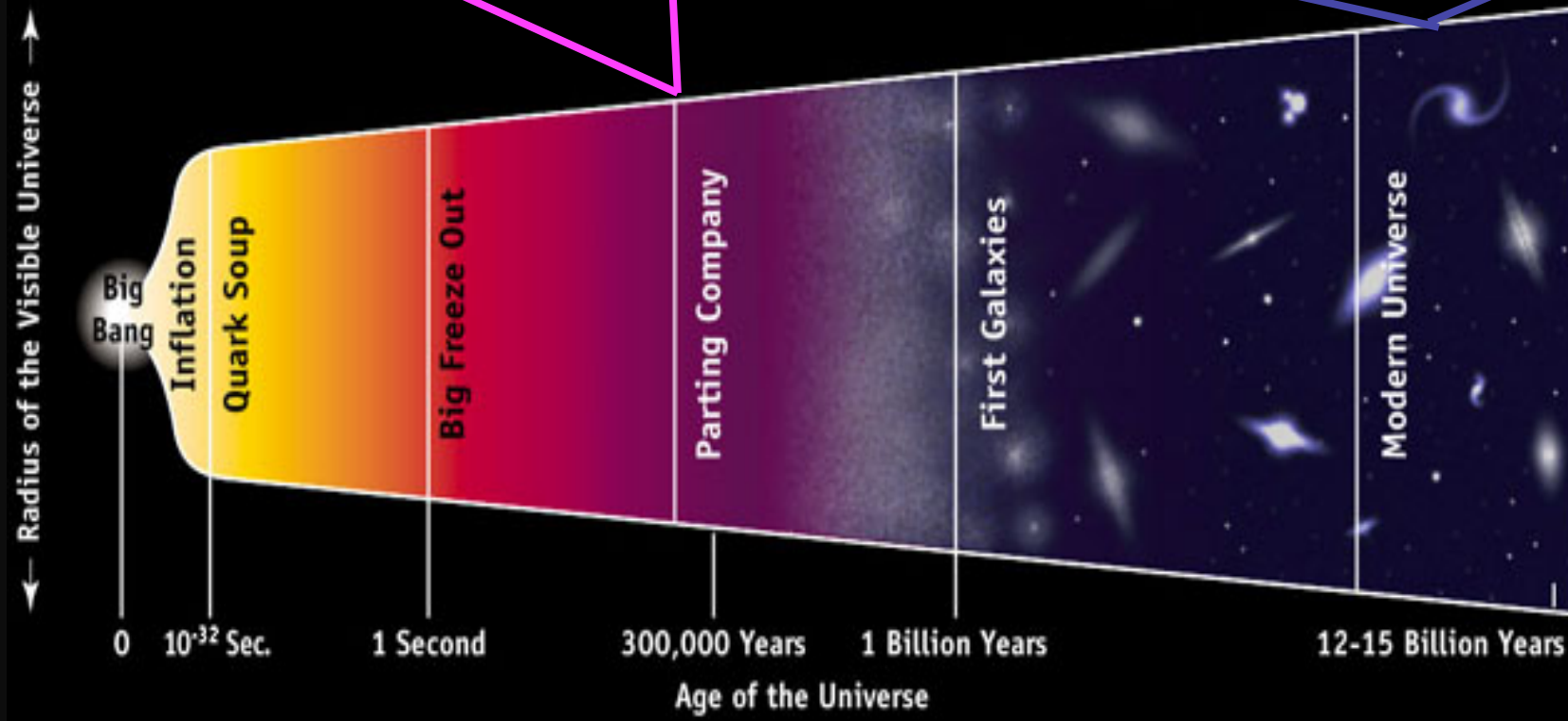
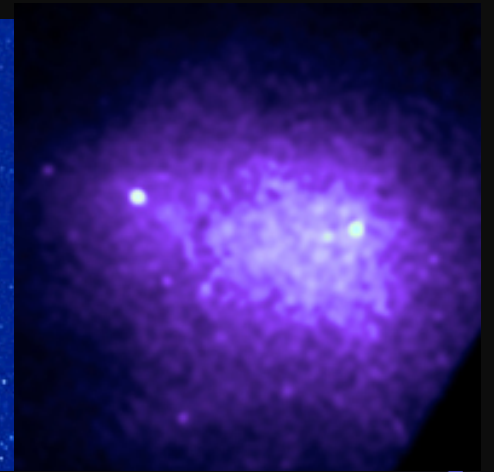
**Stefano Ettori**  
(INAF-OA Bologna)



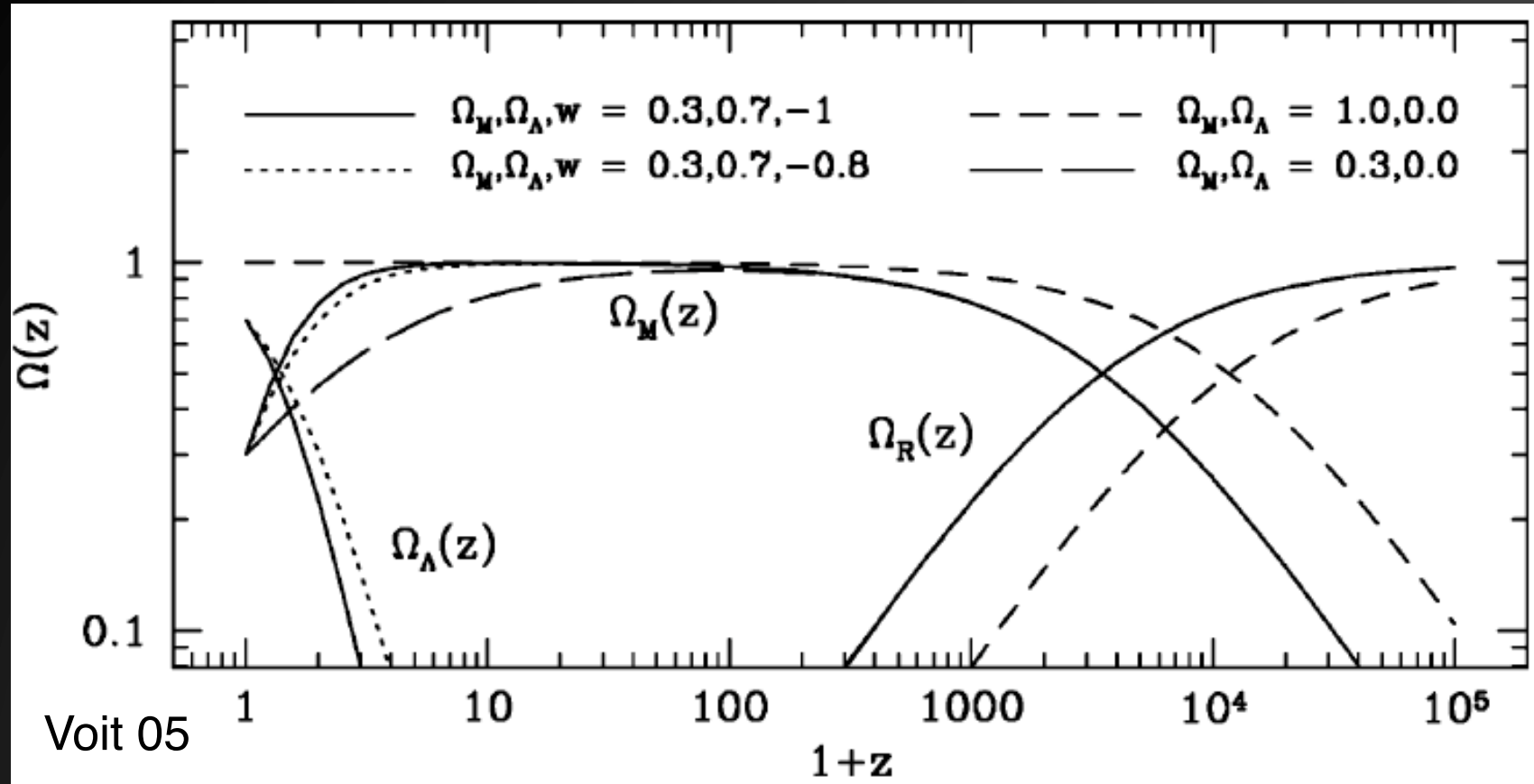
The Planck one-year all-sky survey



(c) ESA, HFI and LFI consortia, May 2010



# Galaxy clusters & cosmology



Matter dominates the dynamics at  $z > 1$

Dark energy (with equation of state  $w = P/\rho$ ) becomes relevant at  $z < 2$

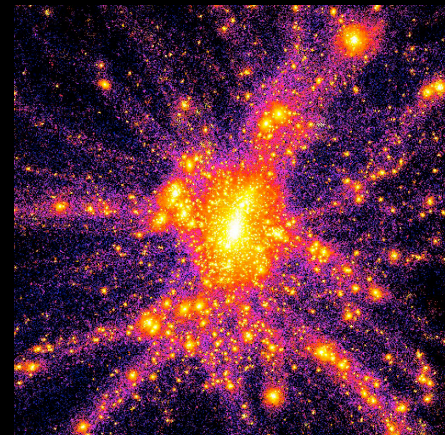
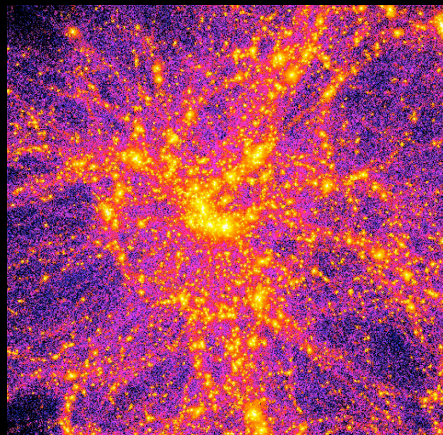
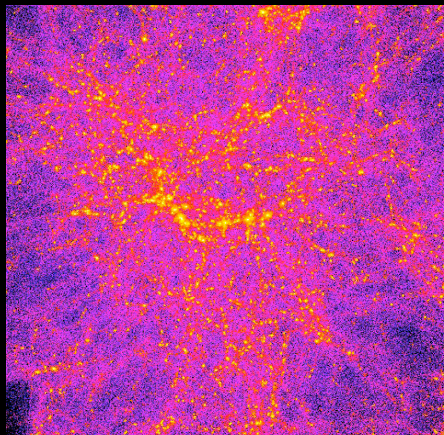
Radiation was the most important component before  $z_{eq} = 2e4 \Omega_m$

z=4

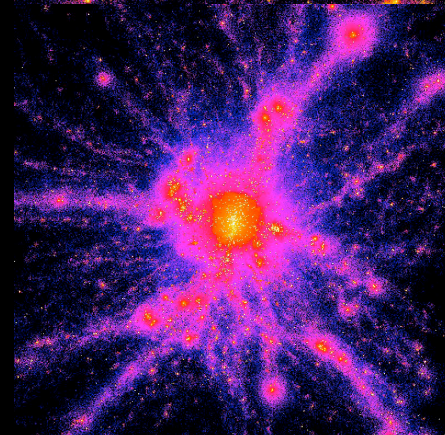
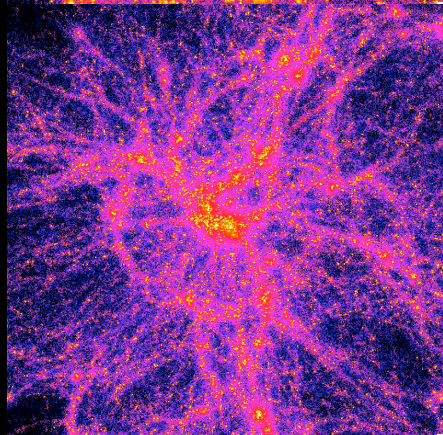
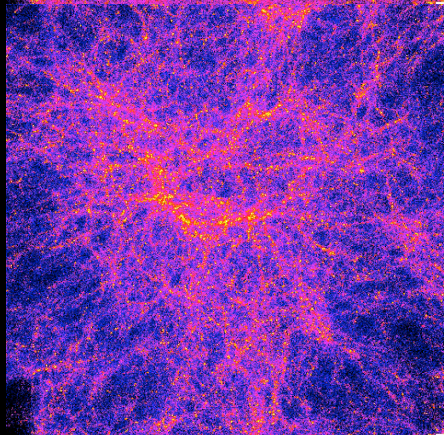
z=2

z=0

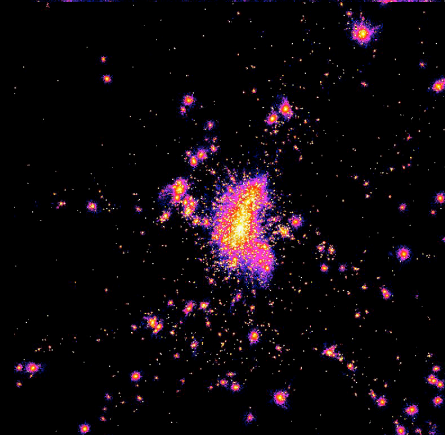
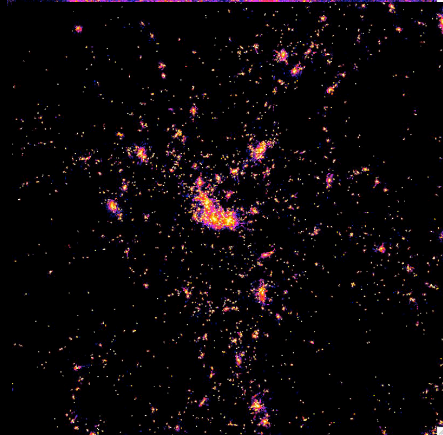
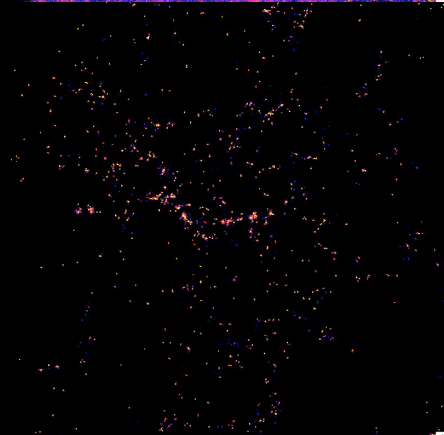
DM



gas



star

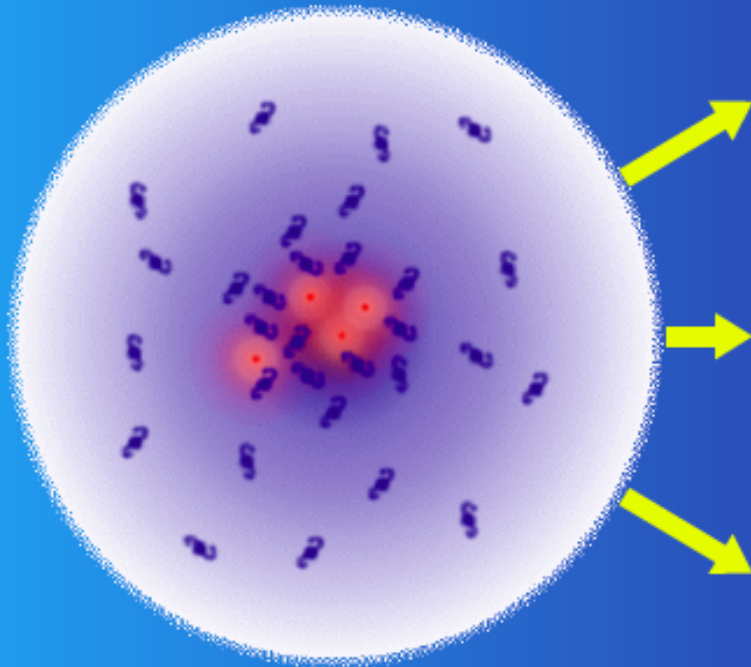


$M_{\text{vir}} \sim 1e15$

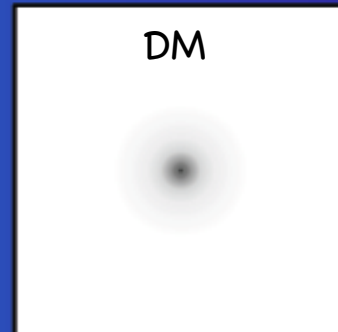
$R_{\text{vir}} \sim 3/h \text{ Mpc}$

# Observable Properties of Clusters

Size:  $\sim 1-5$  Mpc



Mass:  $10^{13} - 10^{15} M_{\odot}$

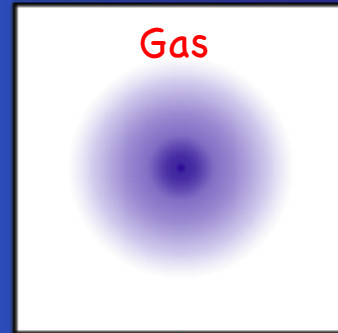


DM

Lensing

Mass distrib./profiles  
Nature ??

Gal dynamics

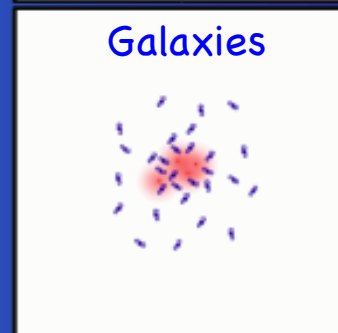


Gas

X-ray

Thermodynamics/masses  
metallicity

SZ effect



Galaxies

Multi- $\lambda$  photometry  
and spectroscopy

Stellar mass/ stellar pop.  
Galaxy evolutions, SF rates

# Galaxy clusters & cosmology

- Concentration of **100–1000** galaxies
- Velocity dispersion (observed):  $\sigma_v \sim 1000 \text{ km s}^{-1}$
- Size:  **$R \sim 1 \text{ Mpc}$**   $\Rightarrow$  the crossing time (lower limit to the relaxation time) is  $t_{\text{cross}} = R/\sigma_v \sim 1 \text{ Gyr} < t_H = 9.8 h^{-1} \text{ Gyr}$   
 $\Rightarrow$  clusters must be dynamically relaxed at the present
- **Mass:** assuming virial equilibrium  $\Rightarrow M \simeq \frac{R\sigma_v^2}{G} \simeq \left(\frac{R}{1}\right) \left(\frac{\sigma_v}{10^3}\right)^2 10^{15} h^{-1} M_\odot$
- Mass components:  $f_{\text{baryons}} \approx 10\text{--}15\%$   
 $(f_{\text{gas}} \approx 10\%, f_{\text{gal}} \approx \text{a few}\%) \Rightarrow f_{\text{DM}} \approx 80\text{--}90\%$
- Intra-Cluster Gas:  $T_X \approx 3\text{--}10 \text{ keV}$ ,  $n_{\text{gas}} \approx 10^{-3} \text{ atoms/cm}^3$ ,  
 **$Z \sim 0.3 \text{ solar}$**   $\Rightarrow$  fully ionized plasma, free-free bremsstrahlung + lines  
emission:  $L_X \sim n_{\text{gas}}^2 \Lambda(T) V \sim 10^{43}\text{--}10^{45} \text{ erg/s}$

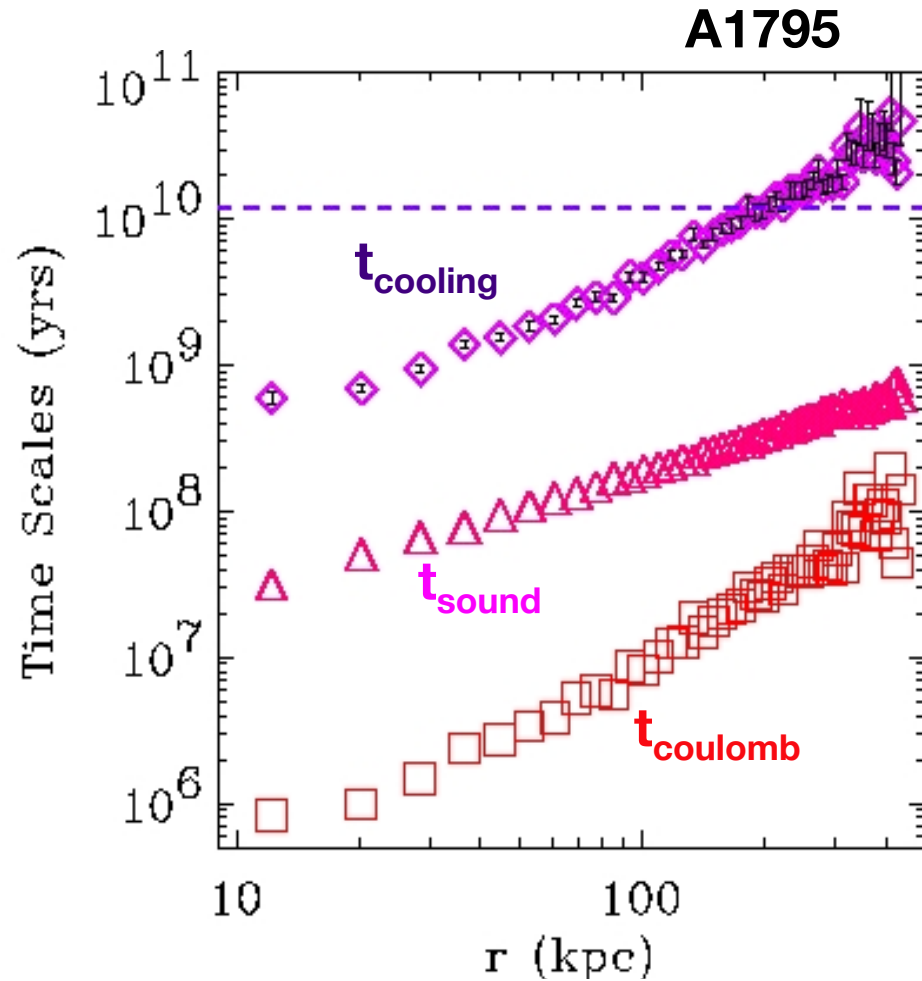
$$k_B T \simeq \mu m_p \sigma_v^2 \simeq 6 \left(\frac{\sigma_v}{10^3}\right)^2 \text{ keV}$$

# X-ray total mass

The ICM is a fluid because the time scale of elastic/Coulomb collisions between ions &  $e^-$  ( $t_{\text{coulomb}} \propto T^{3/2}/n$ ) is  $\ll t_{\text{cooling}} (\propto T^{1/2}/n)$  &  $t_{\text{heating}}$

ICM is in hydrostatic equilibrium:

$$t_{\text{sound}} (\propto R/T^{1/2}) < t_{\text{age}} \approx H_0^{-1}$$



# X-ray total mass

Total mass from X-ray is determined by assuming  
1. spherical symmetry, 2. hydrostatic equilibrium

$$\frac{d\Phi}{dr} = \frac{G M_{tot}(< r)}{r^2} = - \frac{1}{\rho_{gas}} \frac{dP_{gas}}{dr}$$

# X-ray total mass

Total mass from X-ray is determined by assuming  
1. spherical symmetry, 2. hydrostatic equilibrium

$$M_{tot}(< r) = -\frac{kT_{gas}(r) r}{G\mu m_p} \left( \frac{\partial \ln n_{gas}}{\partial \ln r} + \frac{\partial \ln T_{gas}}{\partial \ln r} \right)$$

$$M_{tot}(< r) \propto r \times T_{gas}(r) \times (-\alpha_n - \alpha_T)$$

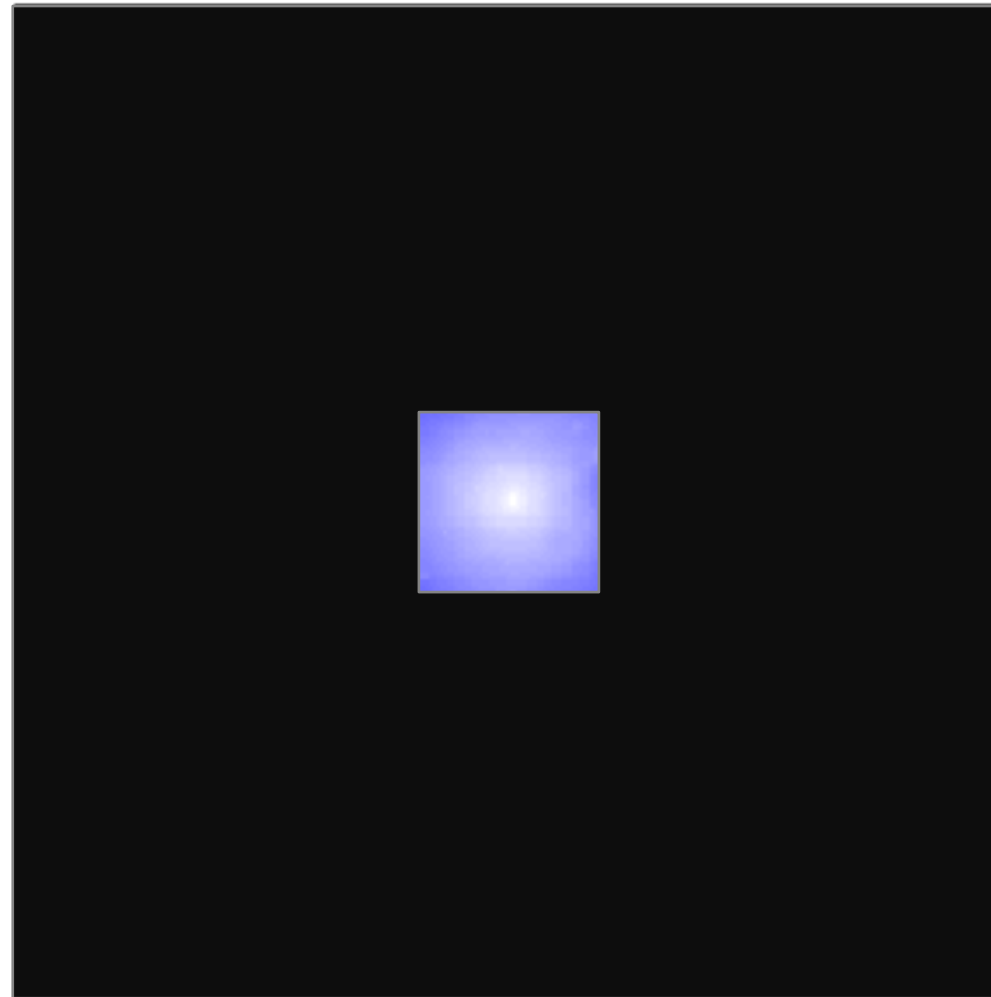
$$\alpha_n \sim -2/-2.4$$

$$\alpha_T \sim 0/-0.8$$

# ICM at $R_{200}$ : $S_b$ of simulated clusters

$R_{2500}$

( $\sim 0.3 R_{200}$   
 $\sim$  CXO limit)



-14

-12

-10

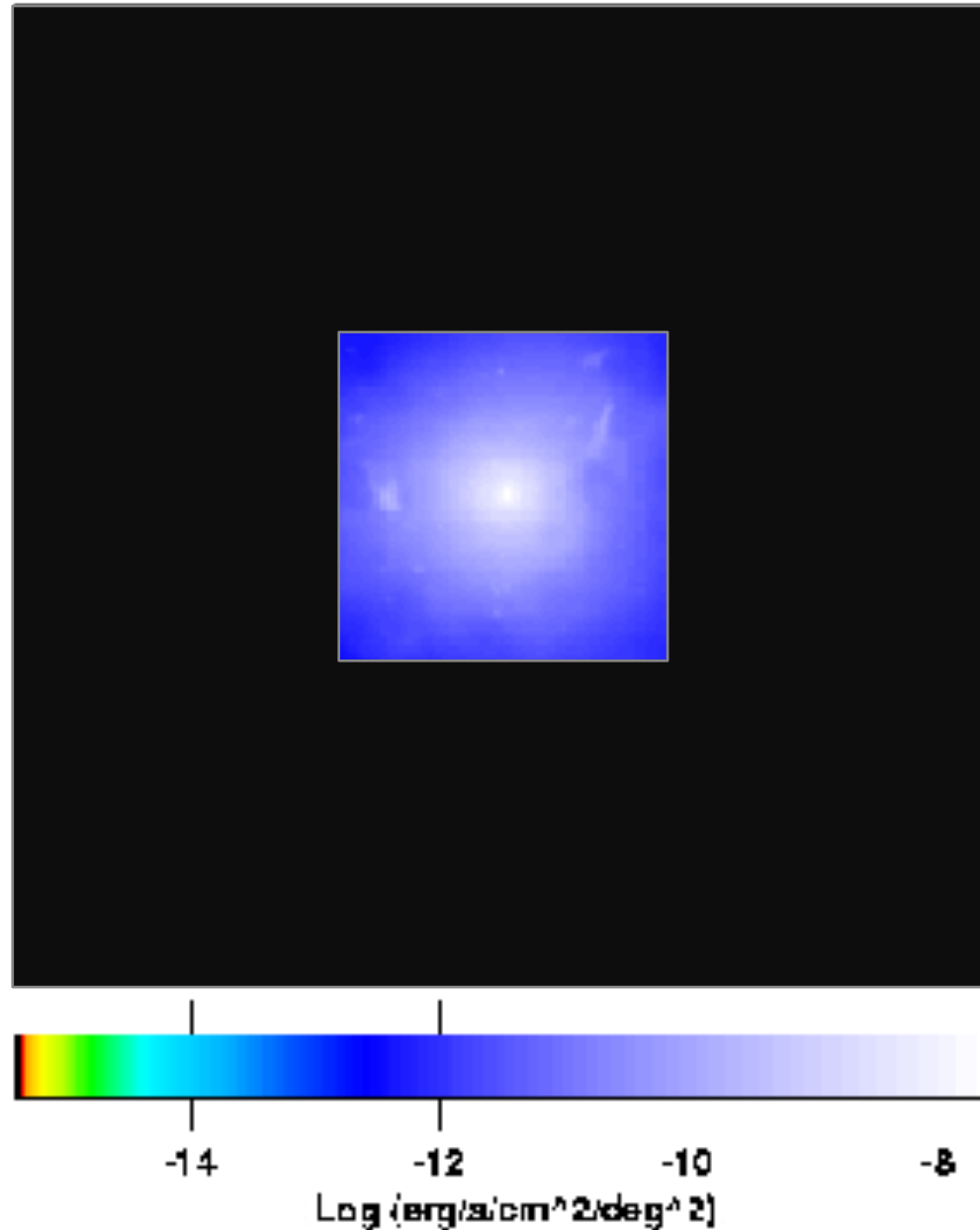
-8

Log (erg/s/cm<sup>2</sup>/deg<sup>2</sup>)

# ICM at $R_{200}$ : $S_b$ of simulated clusters

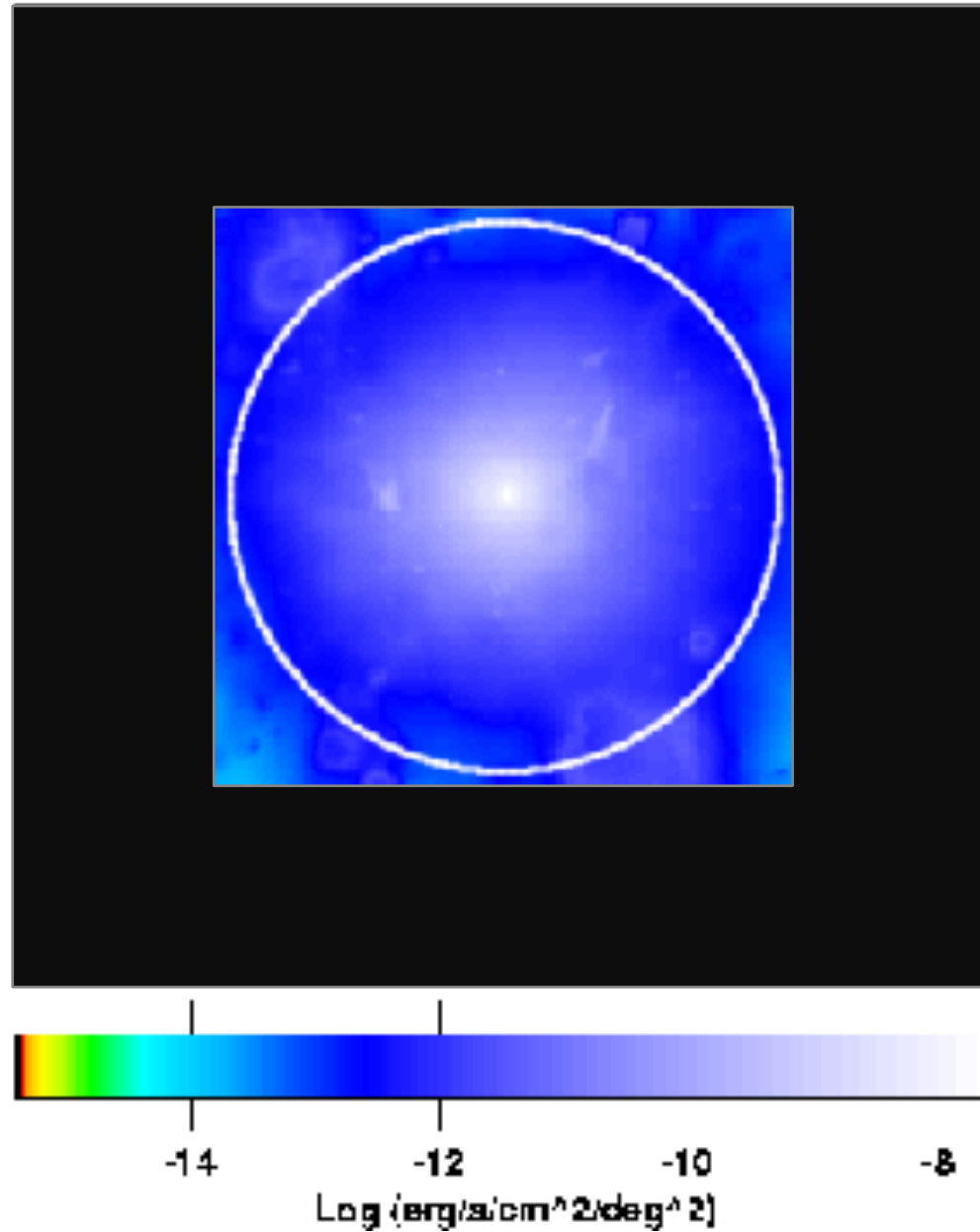
$R_{500}$

( $\sim 0.7 R_{200}$   
~few best  
CXO & XMM  
cases)

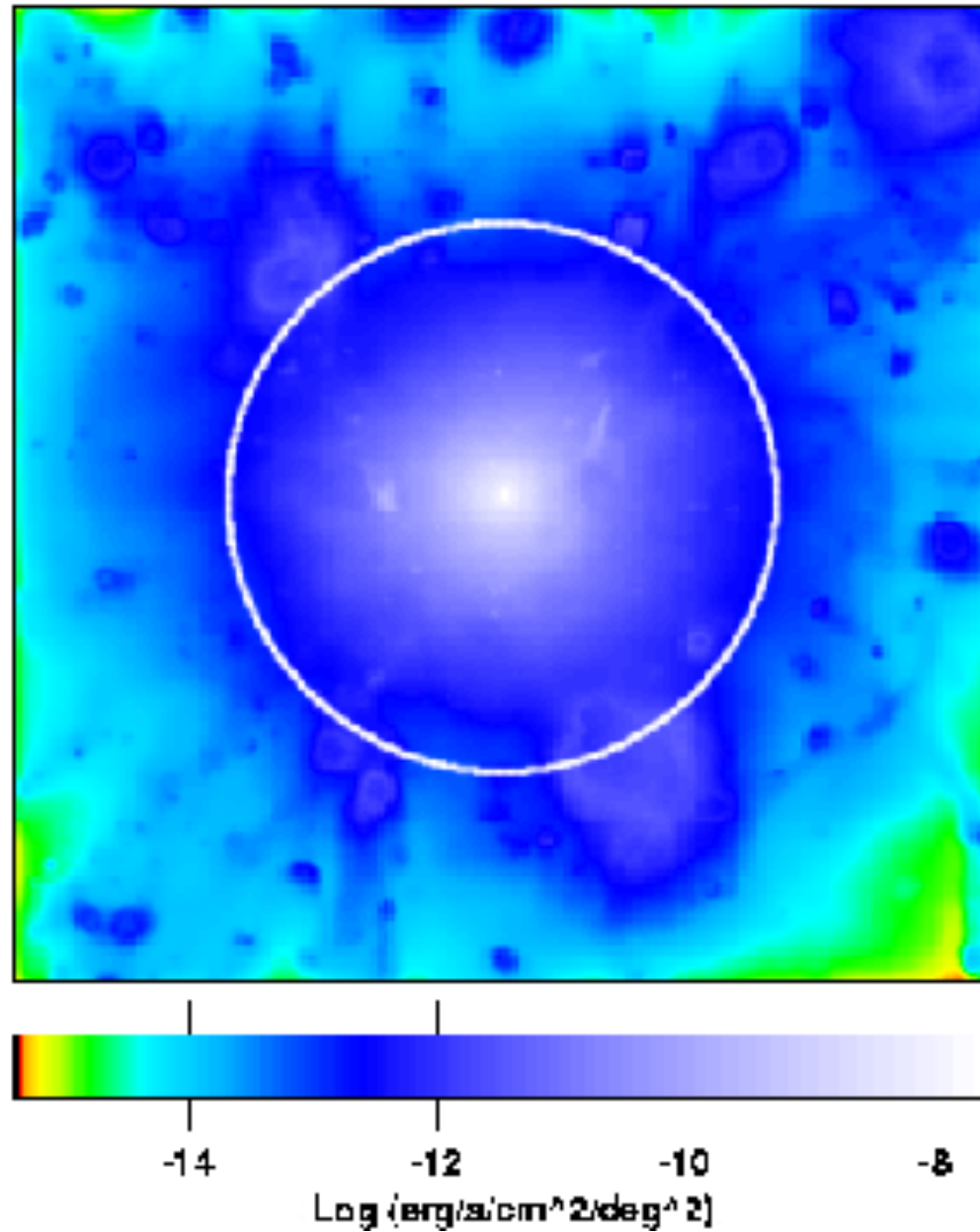


# ICM at $R_{200}$ : $S_b$ of simulated clusters

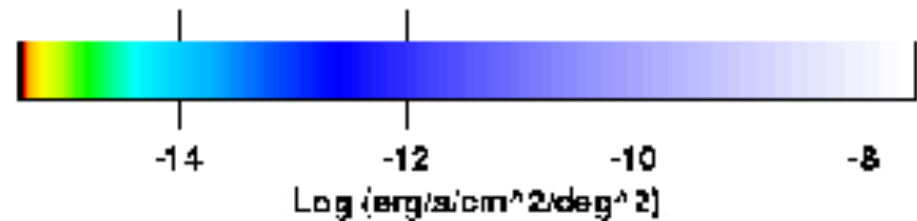
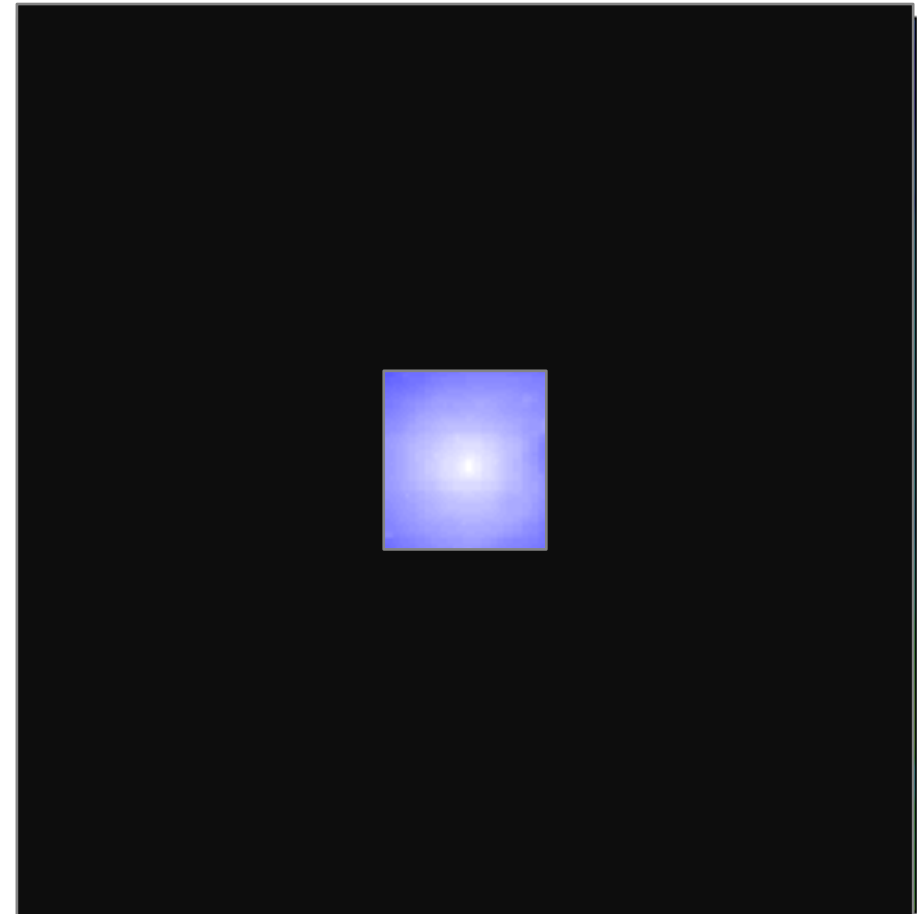
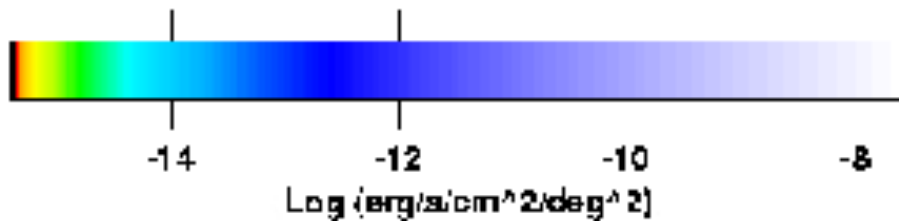
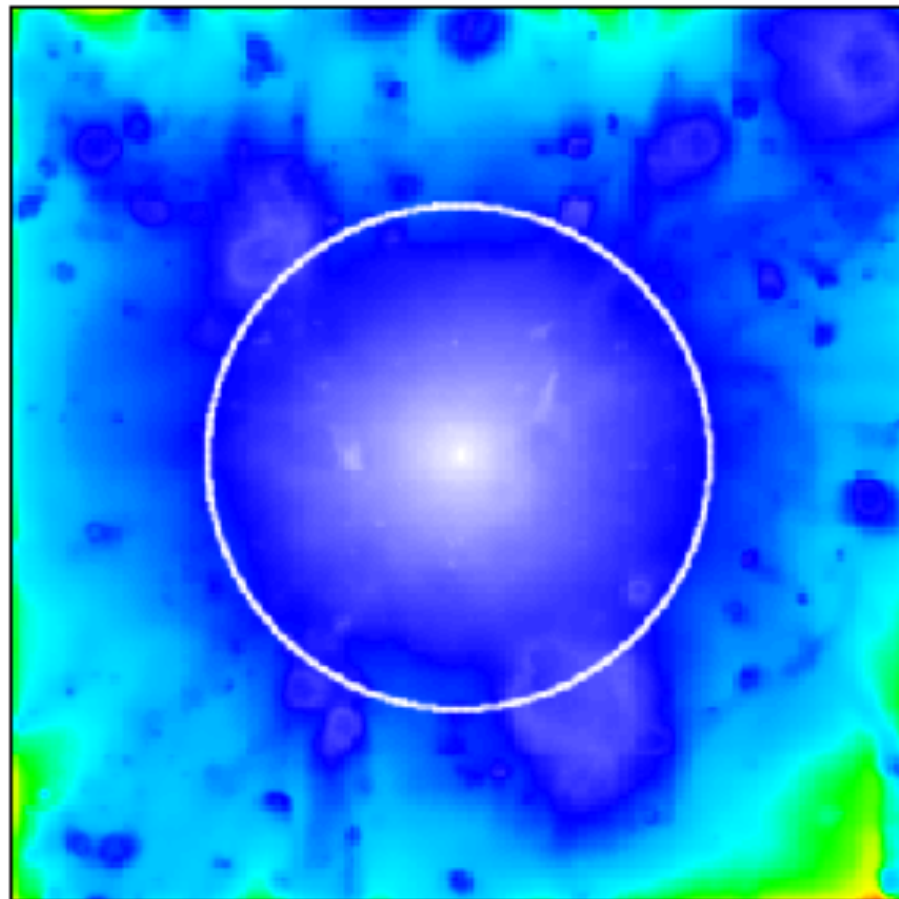
$R_{200}$



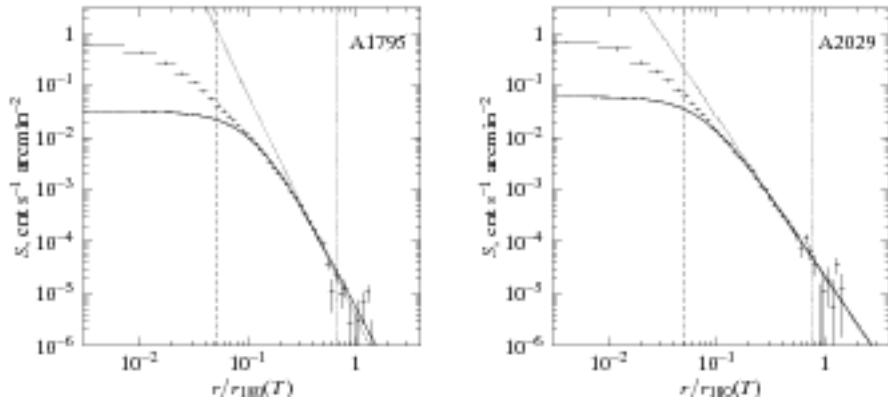
**ICM at  $R_{200}$ :**  $S_b$  of simulated clusters



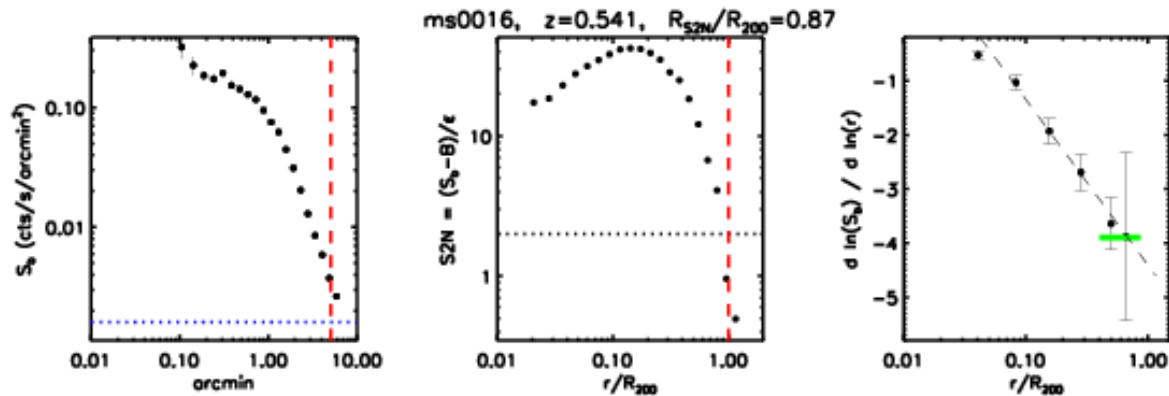
# ICM at $R_{200}$ : $S_b$ of simulated clusters



# $S_b$ at $R_{200}$ : *Observed clusters*



Vikhlinin et al. (99):  $\beta \sim 0.8$  and larger by  $\sim 0.05$  of the global fit value; see also Neumann 2005. Both use a sample of nearby clusters observed with ROSAT/PSPC



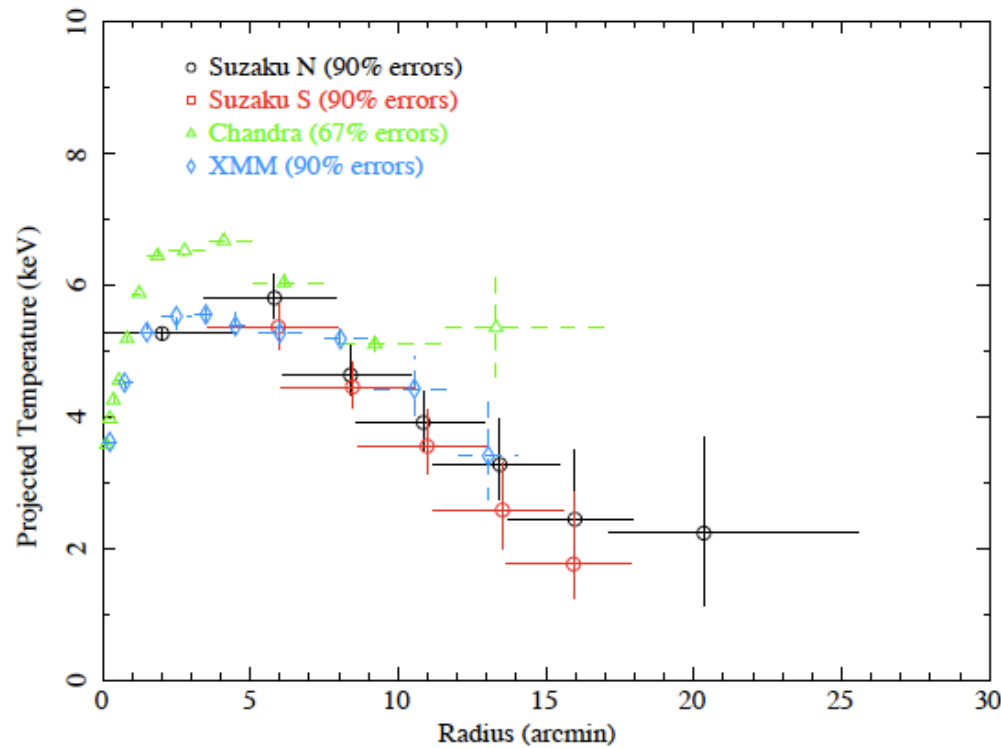
**Study of  $S_b$  at  $r > 0.7 R_{200}$  in a sample of high- $z$  ( $z > 0.3$ ) objects with CXO (Ettori & Balestra 09)**

## *Slope of $S_b$ :*

at  $0.7 R_{200}$ :  $-3.9 \pm 0.7$ , at  $R_{200}$ :  $-4.3 \pm 0.9$

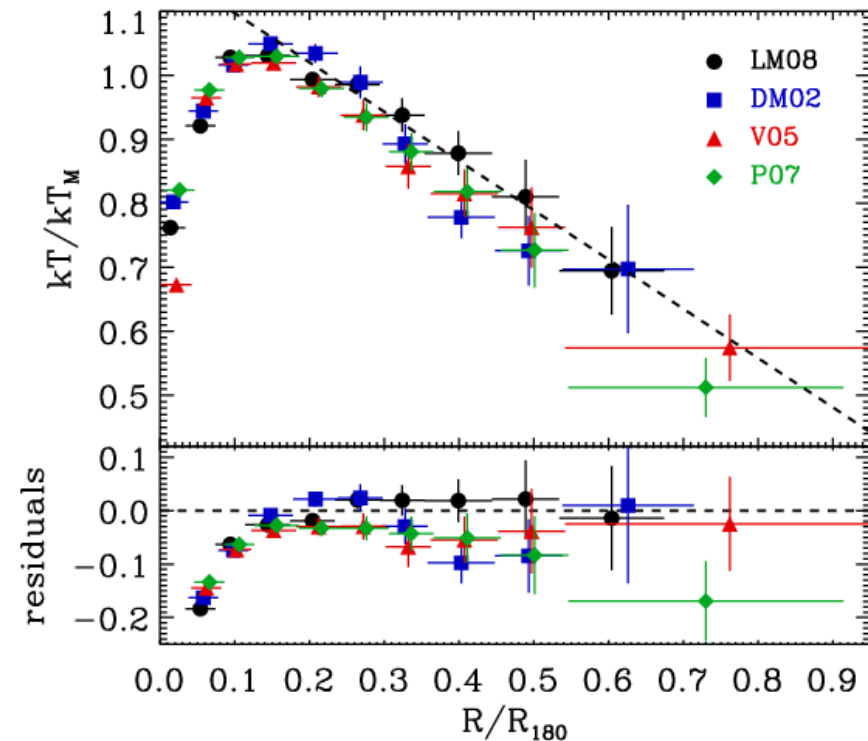
Note:  $S_b \sim r^{1-6\beta}$  ...  $\beta = 0.8/0.9$

# $T_{\text{gas}}$ at $R_{200}$ : *Observed clusters*

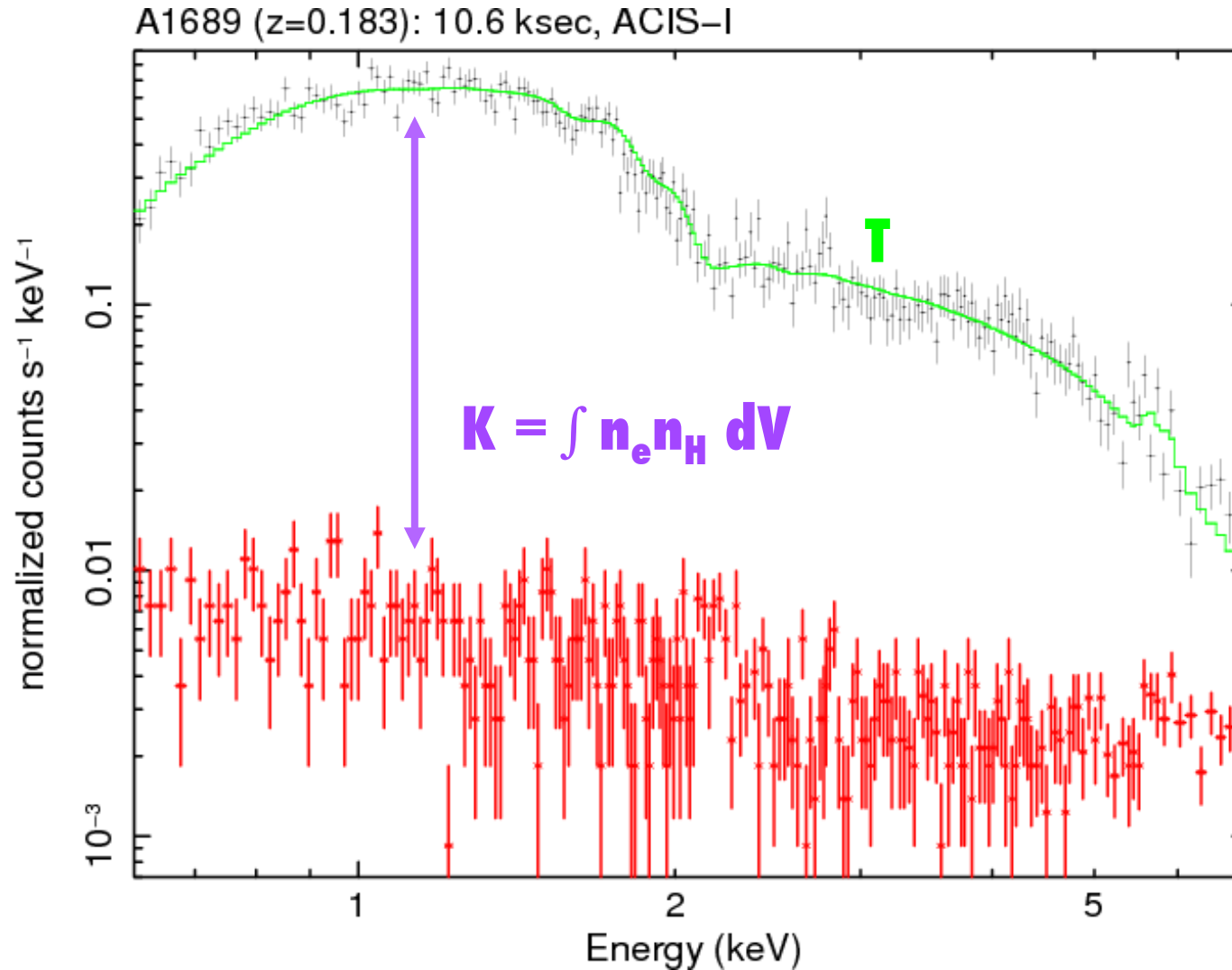


Sample of  $\sim 50$  objects observed with XMM (Leccardi & Molendi 08)

A1795 with *Suzaku* by Bautz et al. (arXiv:0906.3515):  
 $T \sim r^{-0.9}$ ,  $M_{500} \sim 20\text{-}30\% < \text{expected}$



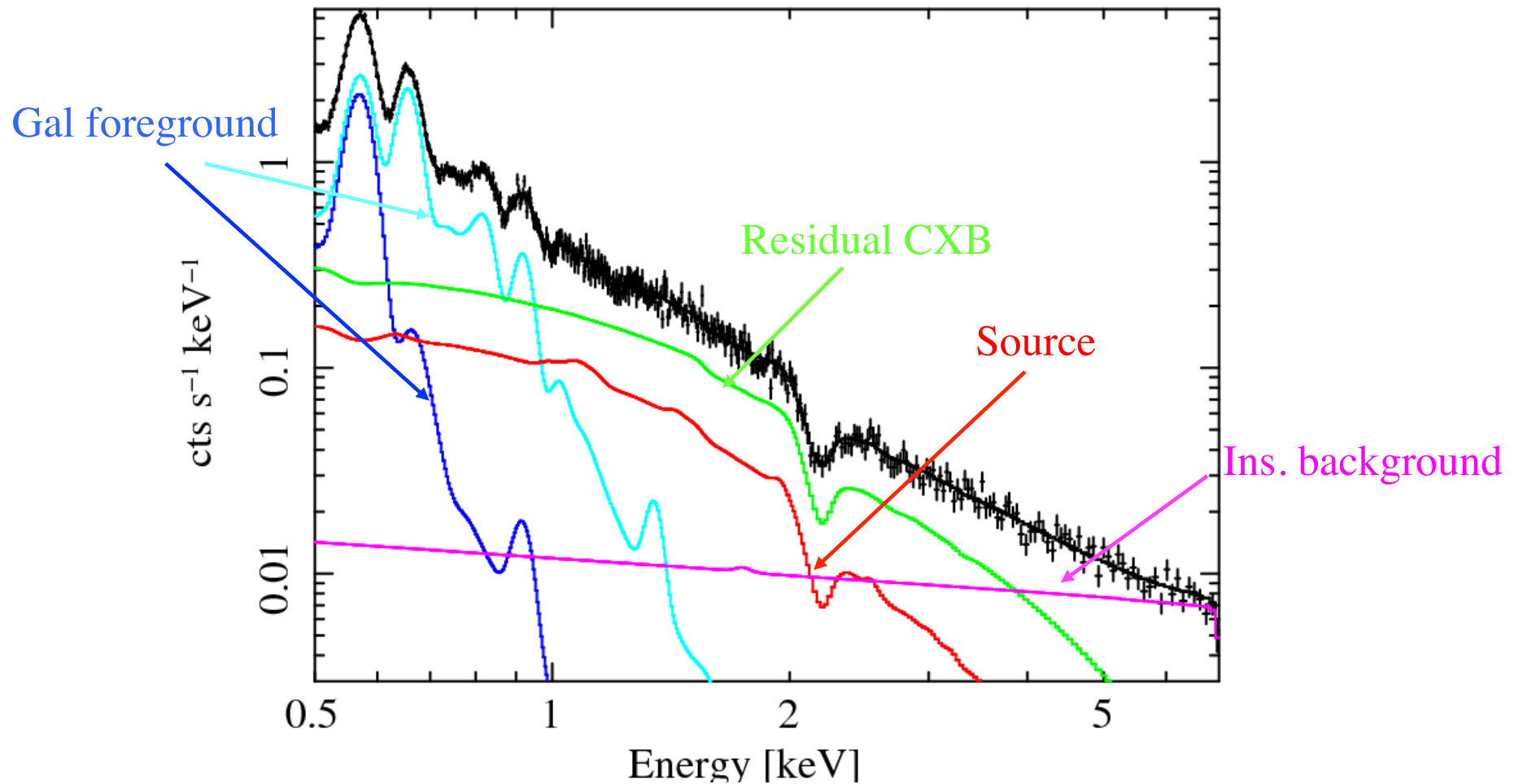
# X-ray total mass: *the observables*



# Bkg: dominant in GCs outskirts

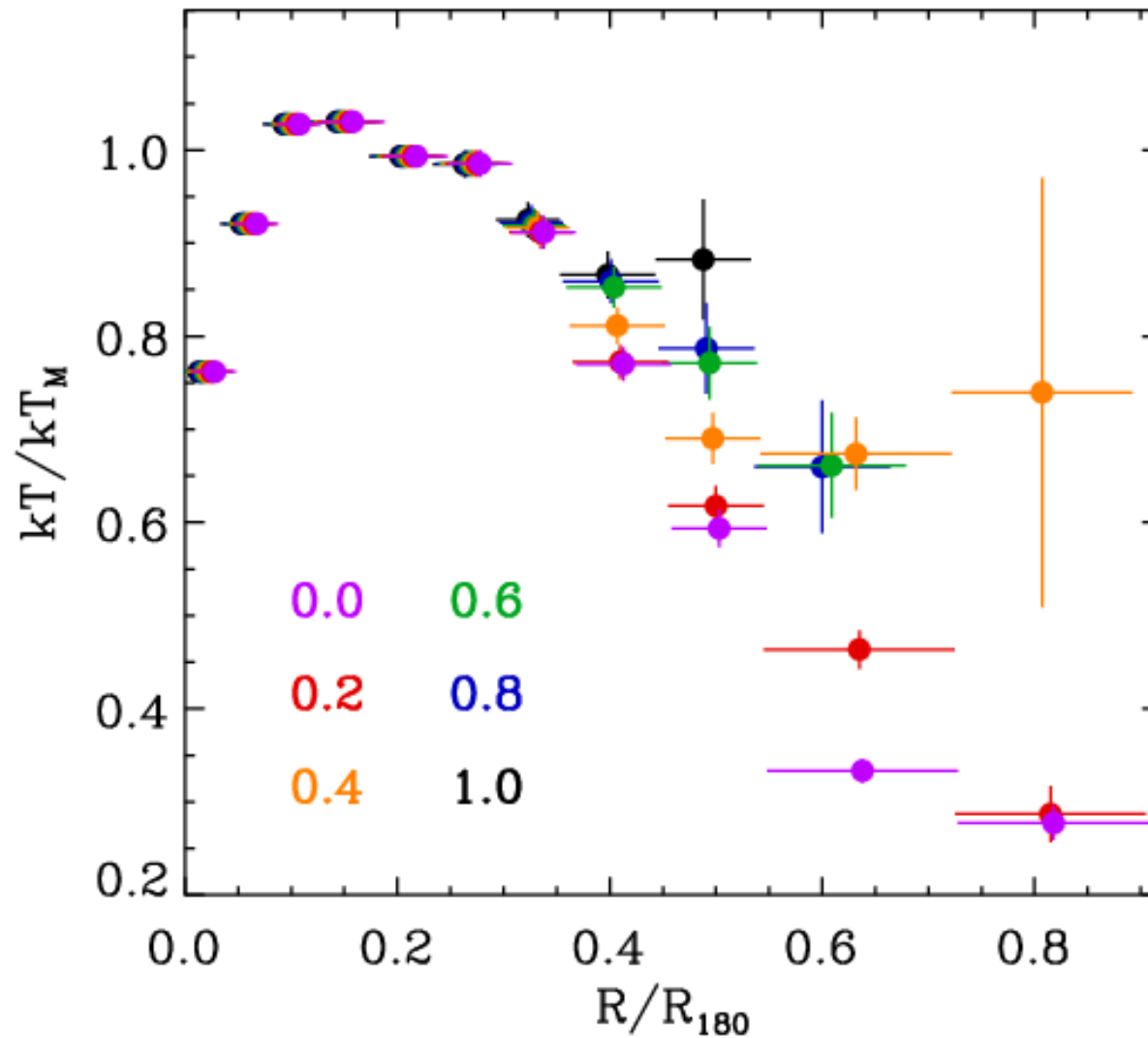
$N_H=0.02$ ,  $T=3$ ,  $A_b=.15$ ,  $z=.035$ ,  $S_b/cgs/amin2=3e-16$   
 $Area/amin2=100$ ,  $texp=1e5$ ,  $f_cxb=0.25$ ,  $f_ins=3.0$

simspec.pha: WFXT data and folded model



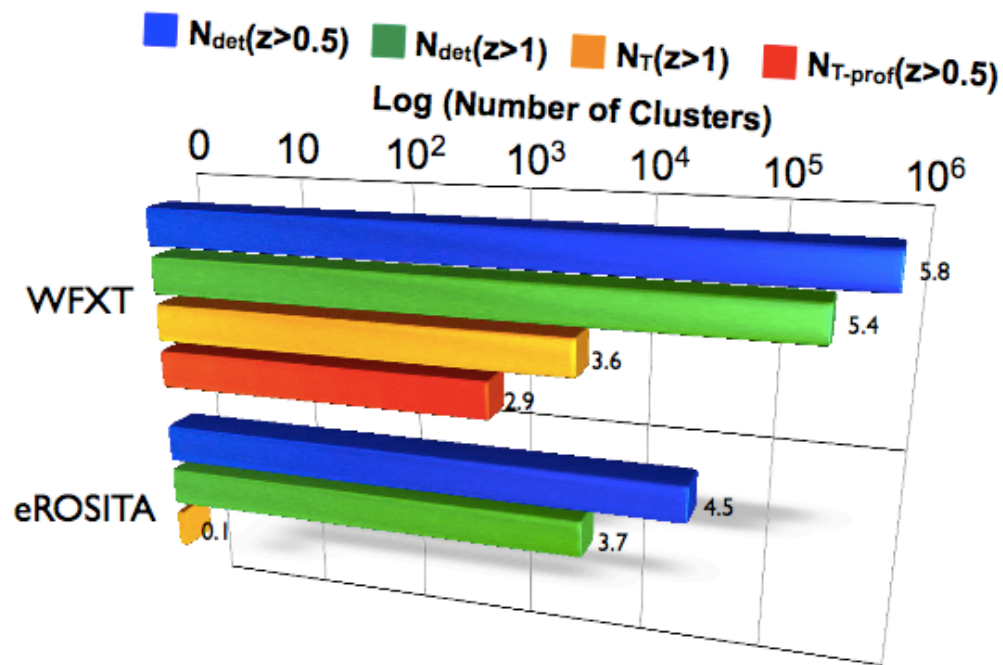
Simulation for 3keV cluster @ R200

# On the Temperature profile

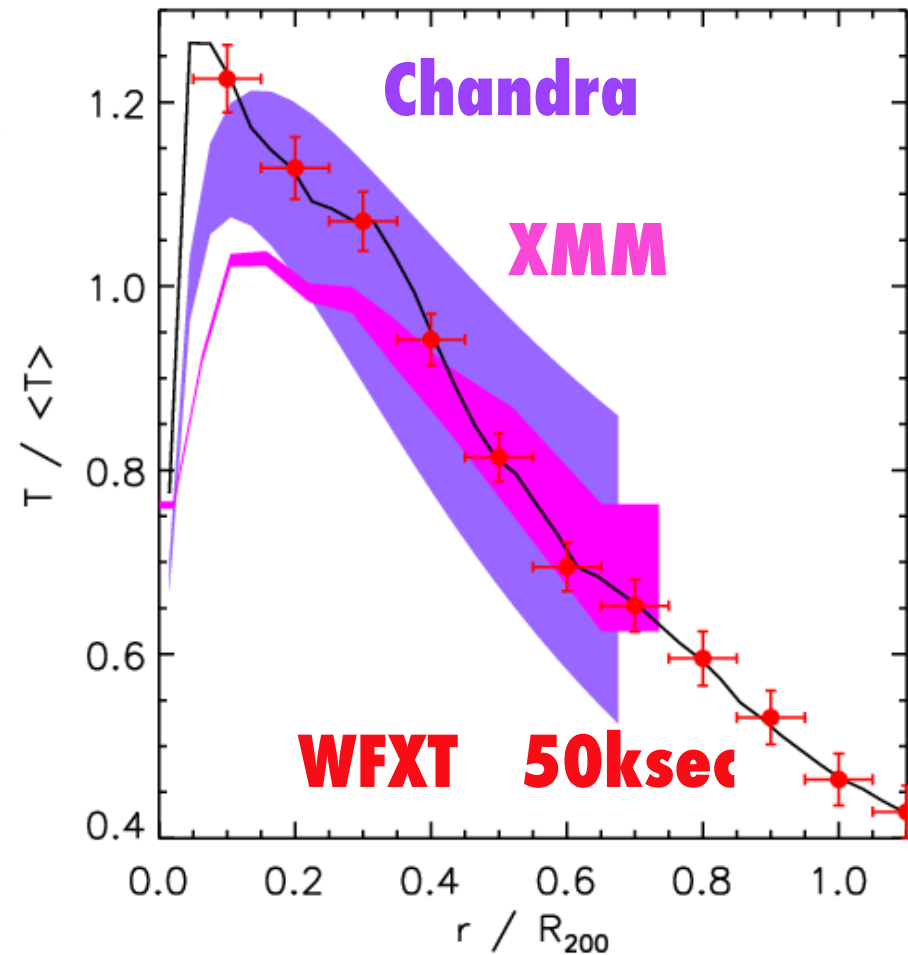


**Changing  $I = \text{Src}/\text{Bkg}$  between 0 and 1  
(Leccardi & Molendi 2008)**

# $T_{\text{gas}}$ profile: *future prospects*



$T(r)$  will be available for 0.1% ( $\sim 1000$ ) of the detected clusters @  $z>0.5$  (Giacconi et al., arXiv:0902.4857)



Ettori & Molendi (arXiv:1005.0382)

# Estimate of the X-ray $M_{\text{tot}}$

- ✓ HEE with functional forms of  $T$  and  $n_{\text{gas}}$  (e.g.  $\beta$ -model) & then fit with mass models (e.g. NFW)

Buote, Pointecouteau, Vikhlinin (& high- $z$  obj with  $T=\text{const}$ )

- ✓ Use of mass models (e.g. NFW) by fitting **either**  $T_{\text{deproj}}$  **or**  $T_{\text{xspec}}$  from inversion of HE

Fabian/Allen, Ettori

- ✓ direct application of HEE on deprojected  $T$  and  $n_{\text{gas}}$

Ettori (and others...)

- ✓ Integral of HEE from deprojected spectra

Nulsen (pioneering work in 1995 with Hans on Virgo)

# Estimate of the X-ray $M_{\text{tot}}$

To summarize: two methods

model-dependent  
**forward**

model-independent  
**backward**

## *Pro*

smooth profiles  
derivable

not need for parameters

## *Contra*

radial shape imposed  
need many parameters  
(e.g. Vikhlinin 05: 10 in  $n_{\text{gas}}$ , 9 in  $T_{\text{gas}}$ )  
degeneracy

radial profiles often not  
smooth enough,  
derivatives problematic

# X-ray total mass in 7 steps

**Step 1:** define a grid in  $\{c, r_s\}$

**Step 2:** define a functional form for

$$M(<r) = K * f(x) * r_s^3 * m(c)$$

$$\text{where } m(c) = \delta/3 * c^3 / (\log(1+c) - c/(1+c))$$

$$f(x) = \log(x + \sqrt{1+x^2}) - x / \sqrt{1+x^2} \quad [\text{Isothermal}]$$

$$= \log(1+x) - x/(1+x) \quad [\text{NFW}]$$

= ...

**Step 3:** at each resolved  $r$ , estimate  $dP = -M/r^2 * n_e * dr$

**Step 4:** define  $P_{\text{out}}$

**Step 5:**  $P(r) = P_{\text{out}} - \text{Sum}(\text{Reverse}(dP))$

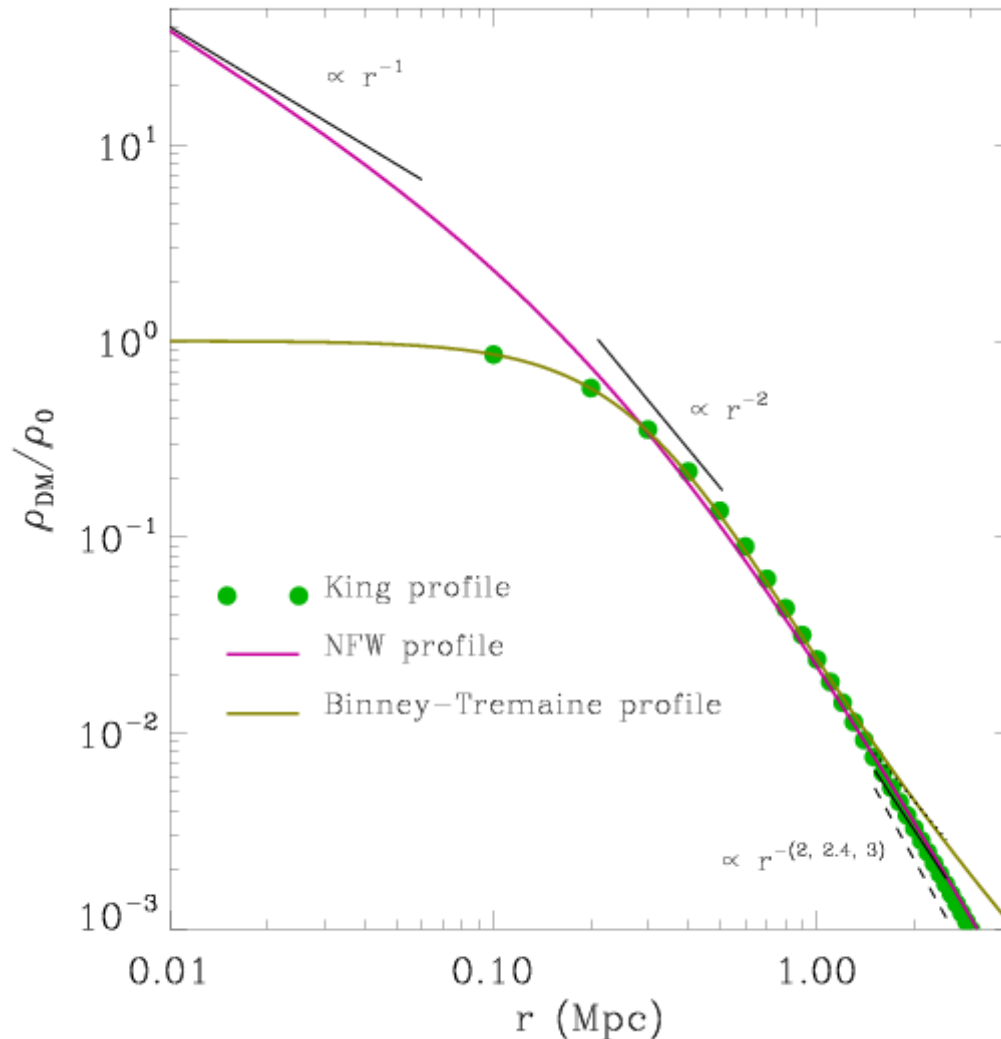
**Step 6:**  $T_{\text{fit}} = P(r) / n_e$

**Step 6bis:** project  $T_{\text{fit}}$  in the observed annulus  
(e.g., with Mazzotta's rule)

**Step 7:**  $\chi^2(c, r_s) = \text{Sum}((T_{\text{fit}} - T_{\text{xspec}})^2 / \text{err}^2)$

# Structure of CDM halos

(Navarro, Frenk, White 1996, 1997)



The **NFW profile** is an approximation to the equilibrium configuration produced in simulations of collisionless DM particles

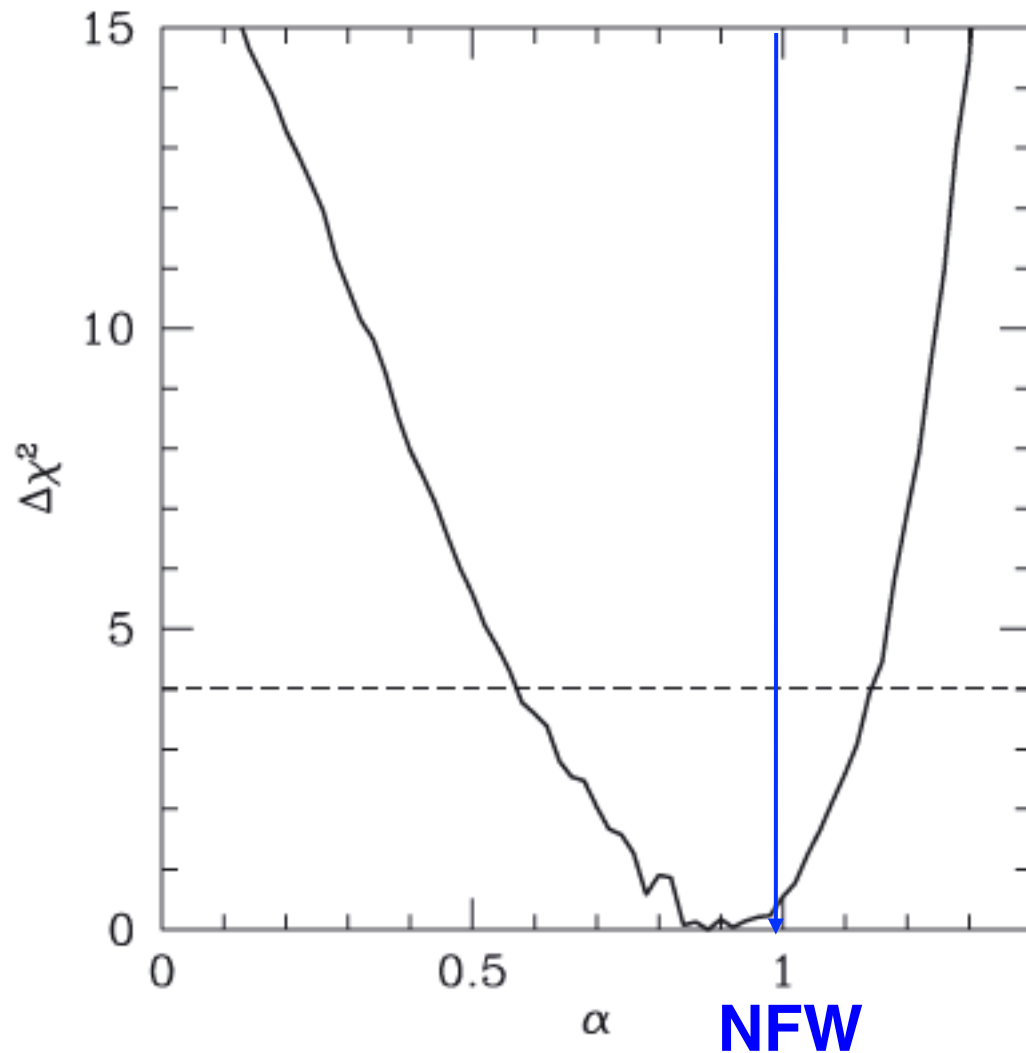
$$\frac{\rho_{DM}}{\rho_0} = \left(\frac{r}{r_s}\right)^{-1} \left(1 + \frac{r}{r_s}\right)^{-2}$$

$$\rho_0 = \rho_c \delta_c$$

$$\delta_c = \frac{200}{3} \frac{c^3}{\ln(1+c) - c/(1+c)}$$

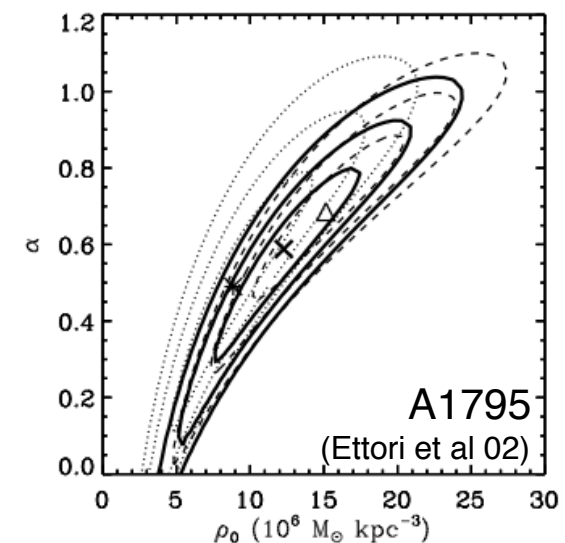
$$R_{200} = M_{200} / (\rho_c V_{200}) = c \times r_s$$

# X-ray mass: *central density slope*

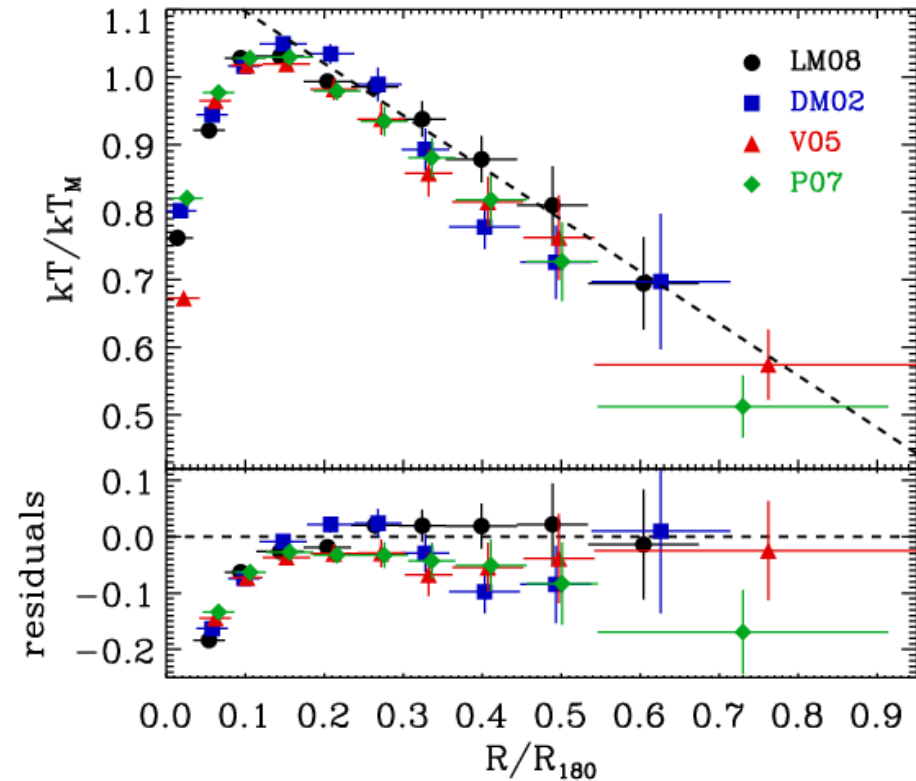
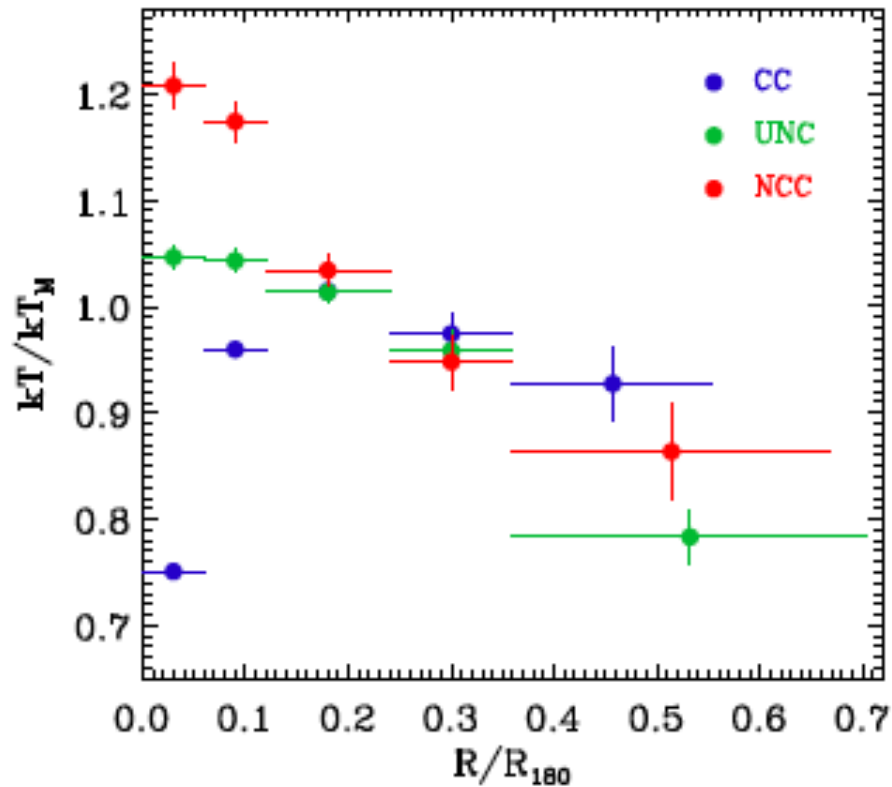


*Schmidt & Allen 07:*  
27 out of 34 clusters  
observed with  
Chandra prefer NFW  
vs isothermal sphere.

Combining the  $\chi^2$ :  
 $\alpha = 0.88 \pm 0.3$  (95% c.l.)



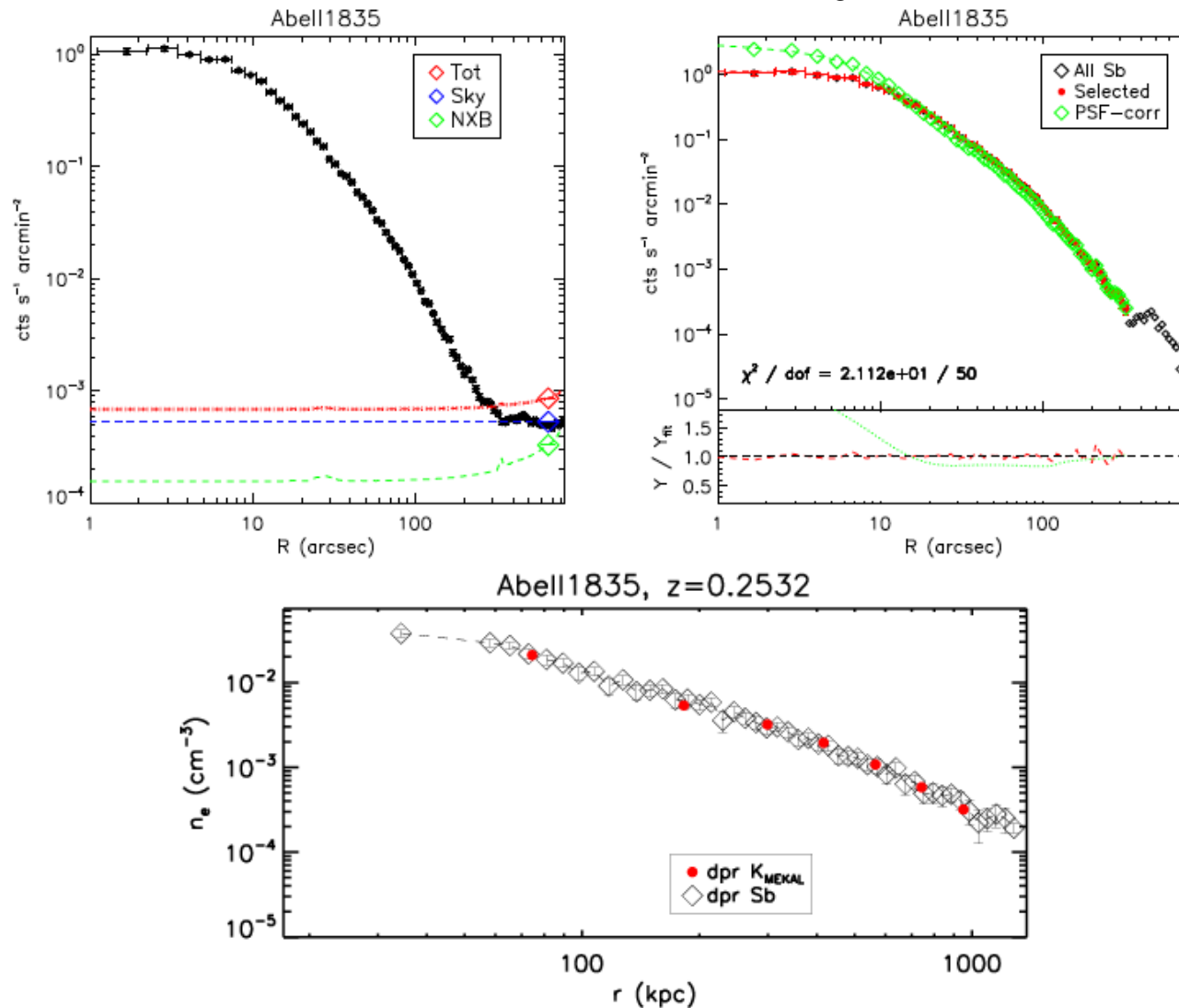
# The sample for $c\text{-}M_{\text{DM}}$ (from Leccardi & Molendi 2008)



44 X-ray luminous galaxy clusters, relaxed (=CC) & not (=NCC), observed with *XMM-Newton* in the z-range 0.1–0.3

# The sample

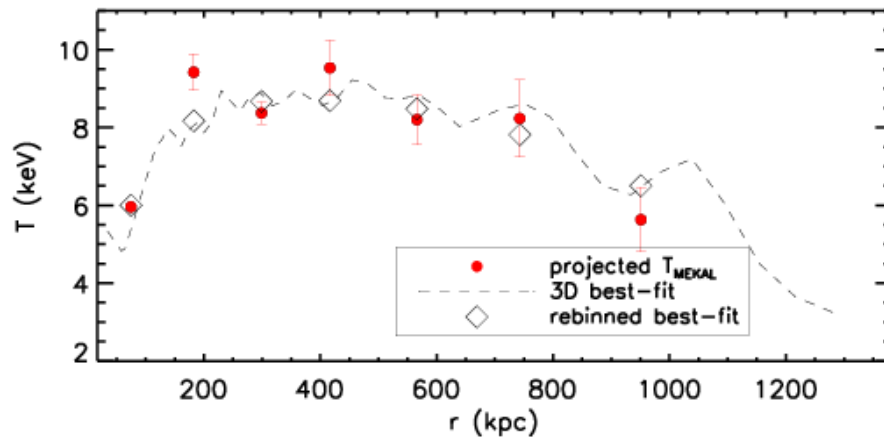
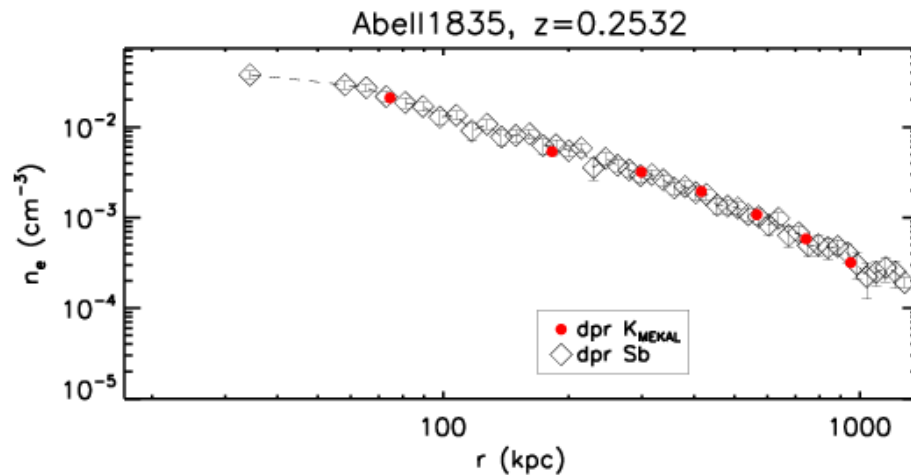
We have extended the LM08 spectral analysis with an analysis of the XMM  $S_b$  to recover  $n_{\text{gas}}$



# The analysis

We have extended the LM08 spectral analysis with an analysis of the XMM  $S_b$  to recover  $n_{\text{gas}}$

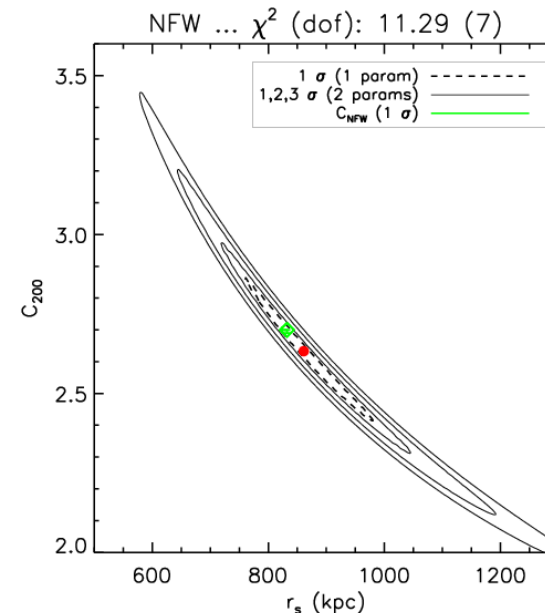
We use  $n_{\text{gas}}$  &  $T_{\text{gas}}$  +NFW to constrain  $\{r_s, c\}$



$$M_{\text{DM}}(< r) = M_{\text{tot}}(< r) - M_{\text{gas}}(< r) = 4\pi r_s^3 \rho_s f(x),$$

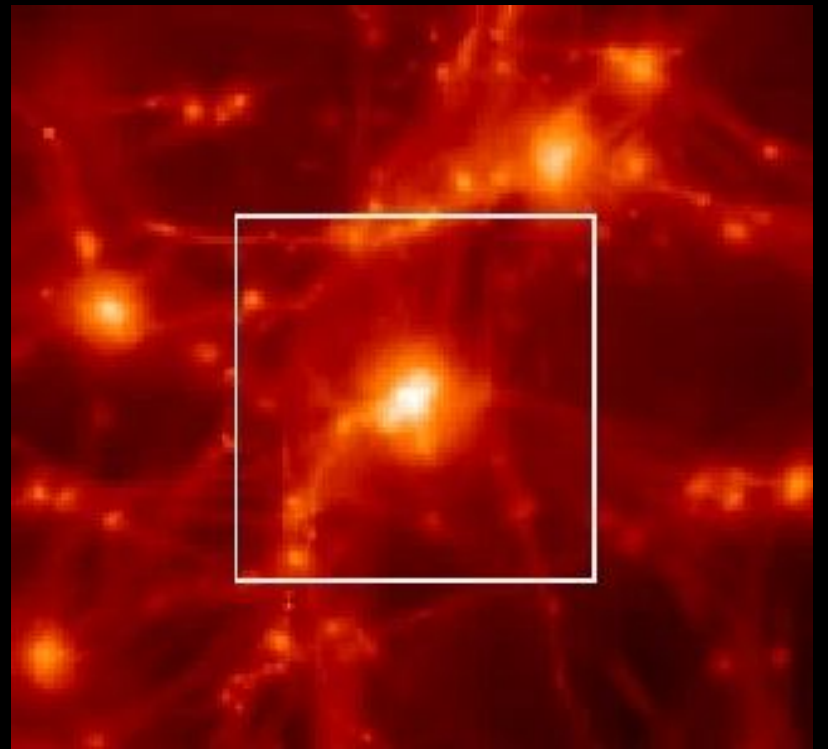
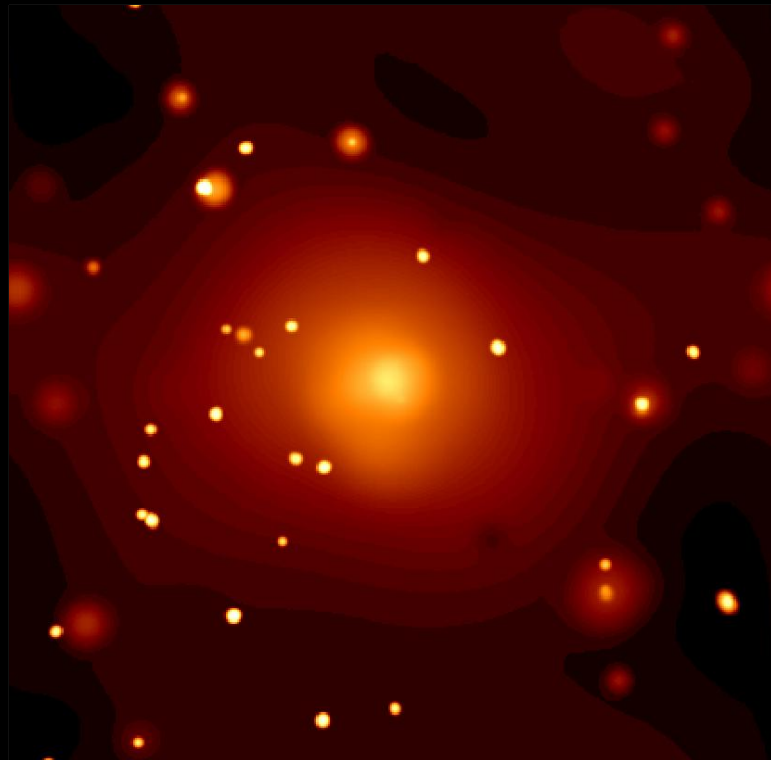
$$\rho_s = \rho_{c,z} \frac{200}{3} \frac{e^3}{\ln(1+c) - c/(1+c)}$$

$$f(x) = \ln(1+x) - \frac{x}{1+x} \quad (1)$$



# But do we know the systematics in the estimates of $M_{\text{tot}}$ in X-ray galaxy clusters ?

Evrard, Metzler, Navarro 96; Schindler 96; Bartelmann & Steinmetz 96;  
Balland & Blanchard 97; Kay et al. 04; **Rasia, SE et al. 06**; Hallman et al. 06;  
Nagai, Vikhlinin, Kravtsov 07; **Meneghetti, Rasia, SE et al. 2010**

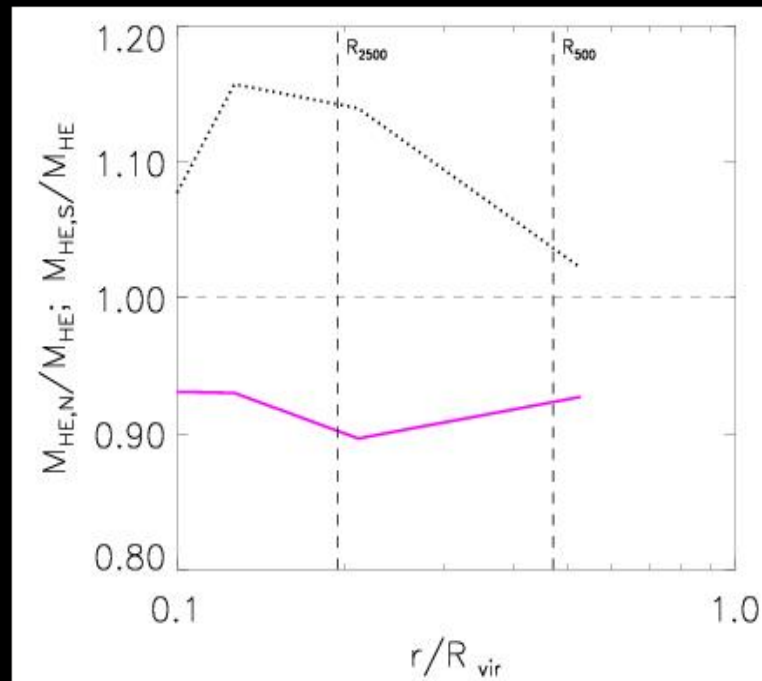
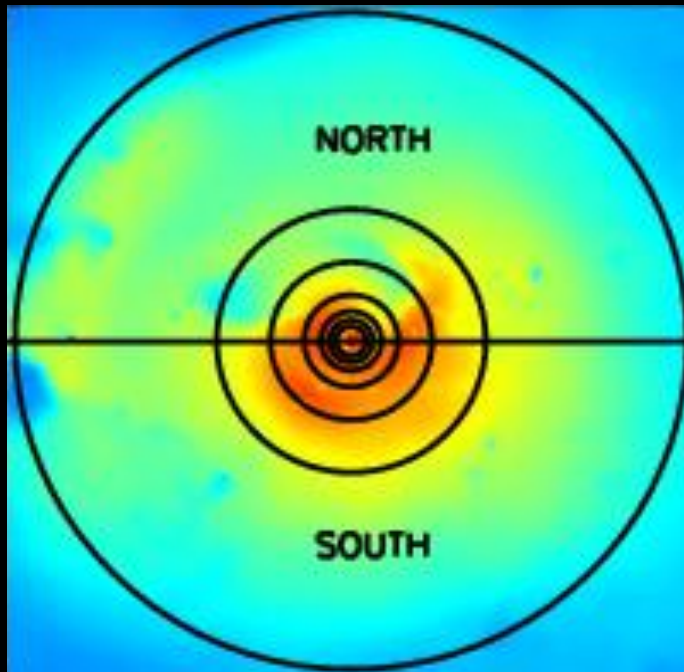


# X-ray total mass: results

X-ray  $M_{\text{est}}$  underestimates  $M_{\text{true}}$  by 10-45 %

→ ~ half of the error budget comes from neglecting gas motions

→ inhomogeneities in T map affect  $M_{\text{tot}}$  by 10-15 %



# X-ray total mass: results

**X-ray  $M_{\text{est}}$  underestimates  $M_{\text{true}}$  by 10-45 %**

**→ ~ half of the error budget comes from neglecting gas motions**

**→ inhomogeneities in T map affect  $M_{\text{tot}}$  by 10-15 %**

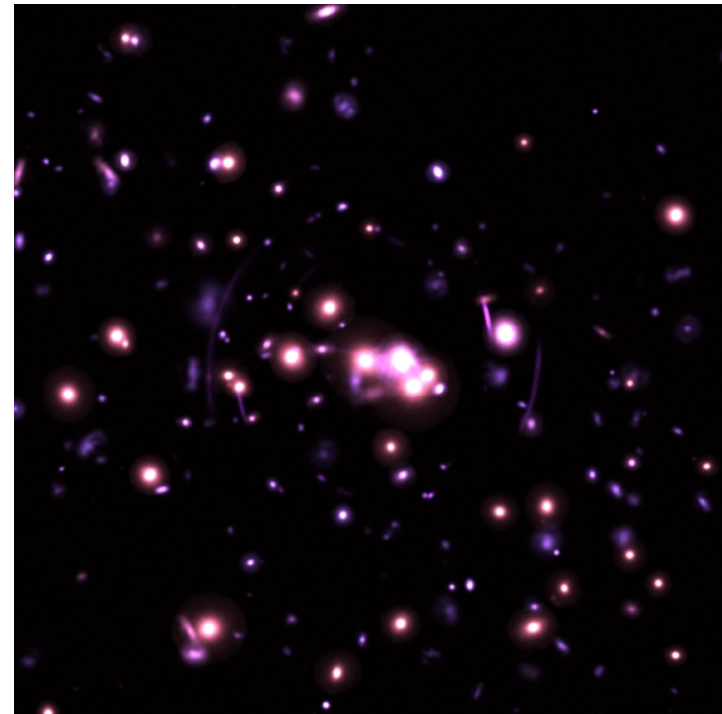
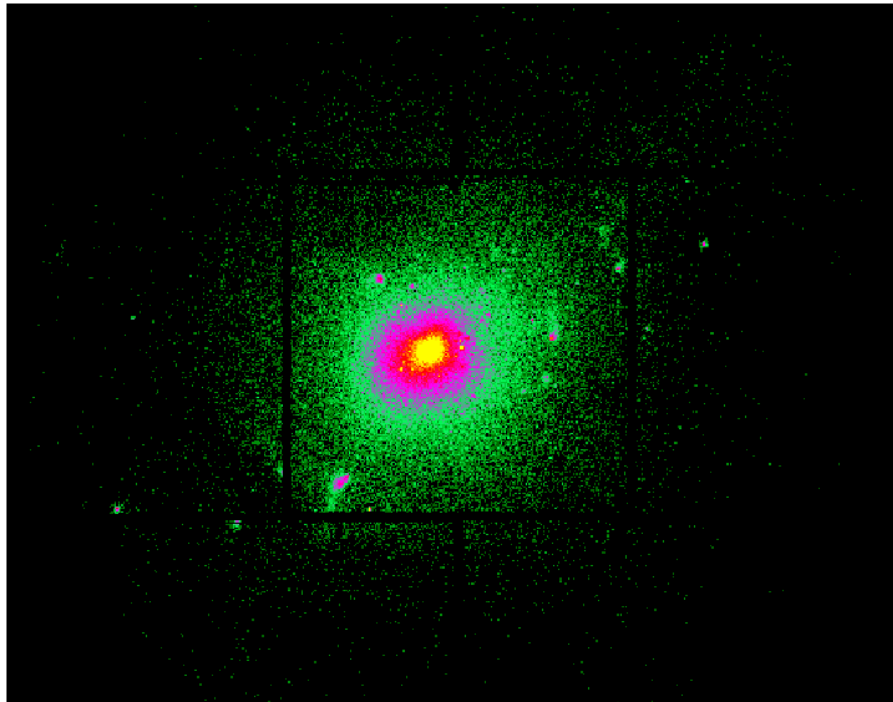
**→ poor constraints on  $n_{\text{gas}}$  from  $\beta$ -model; due to the limited radial interval over which the fit is done,  $\beta$  /  $c_{\text{NFW}}$  are always **lower** / **higher** than the values measured from fit of  $\rho_{\text{gas}}$  up to  $R_{200}$**

# X-ray vs lensing mass: *simulations*

$M_x$  / X-MAS &  $M_{\text{lens}}$  / SkyLens

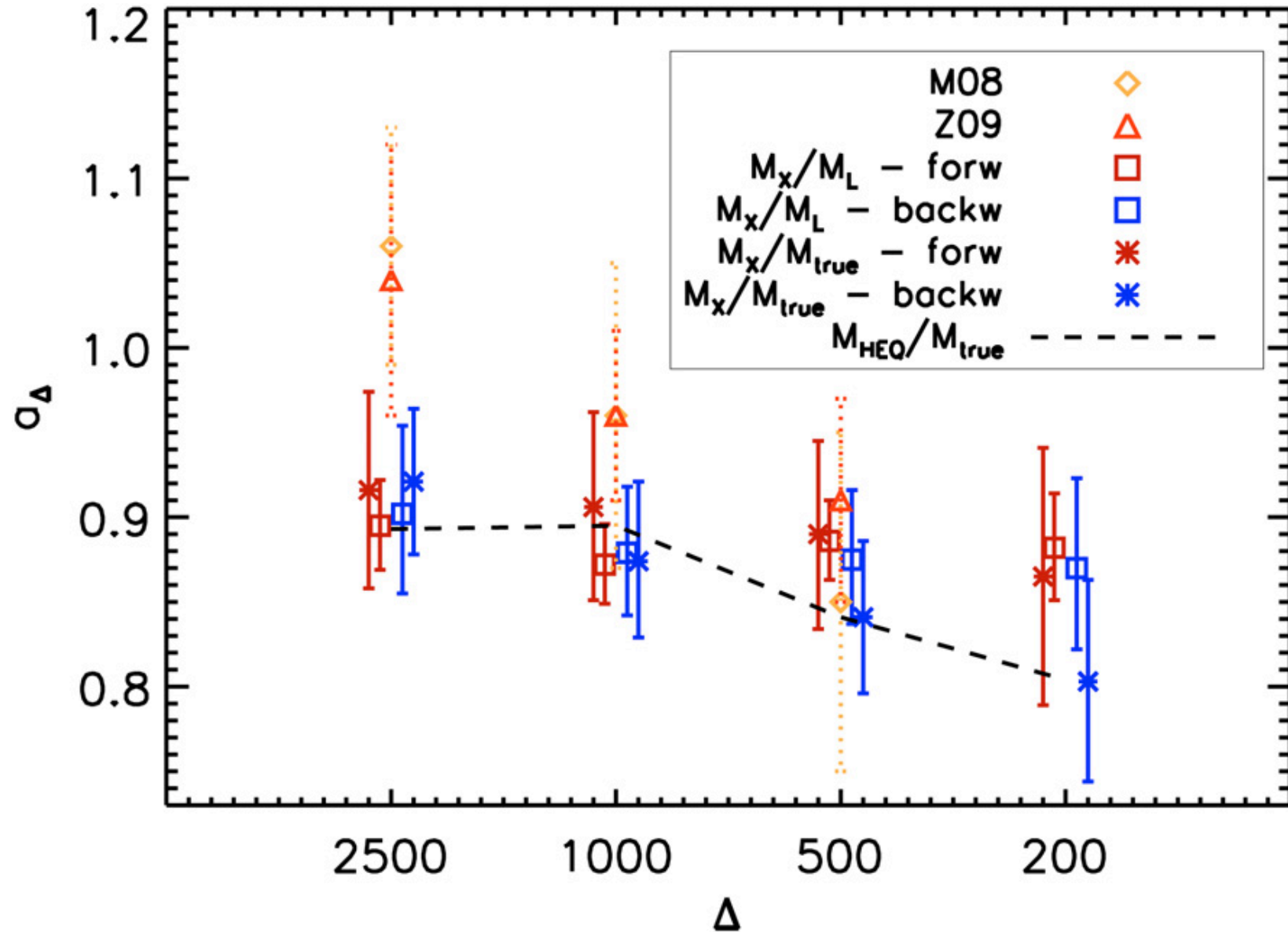
both convolve hydro simulations with observational setup

(work with E. Rasia & M. Meneghetti;  
see also Nagai, Kravtsov, et al.)

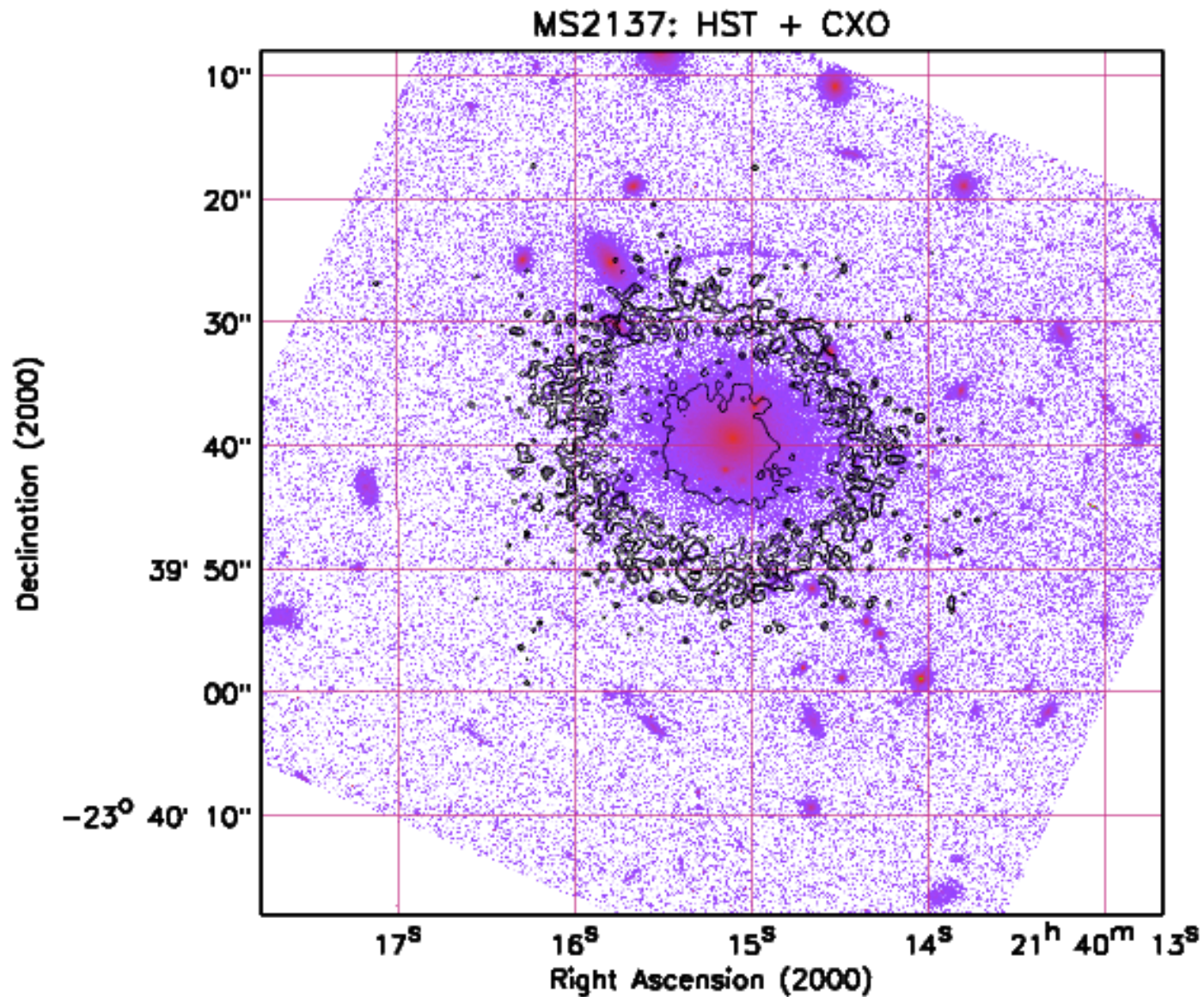




# X-ray vs lensing mass: *simulations*

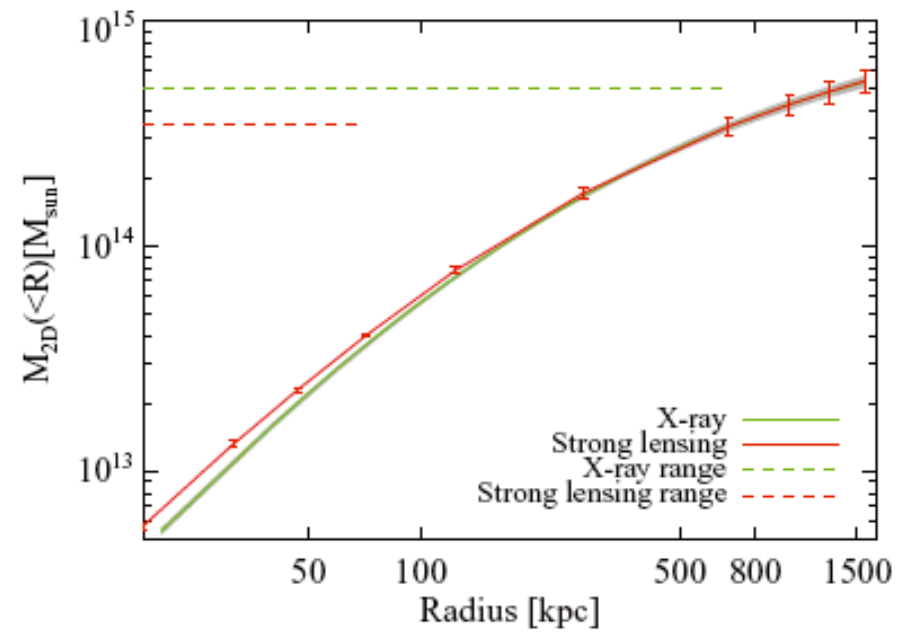
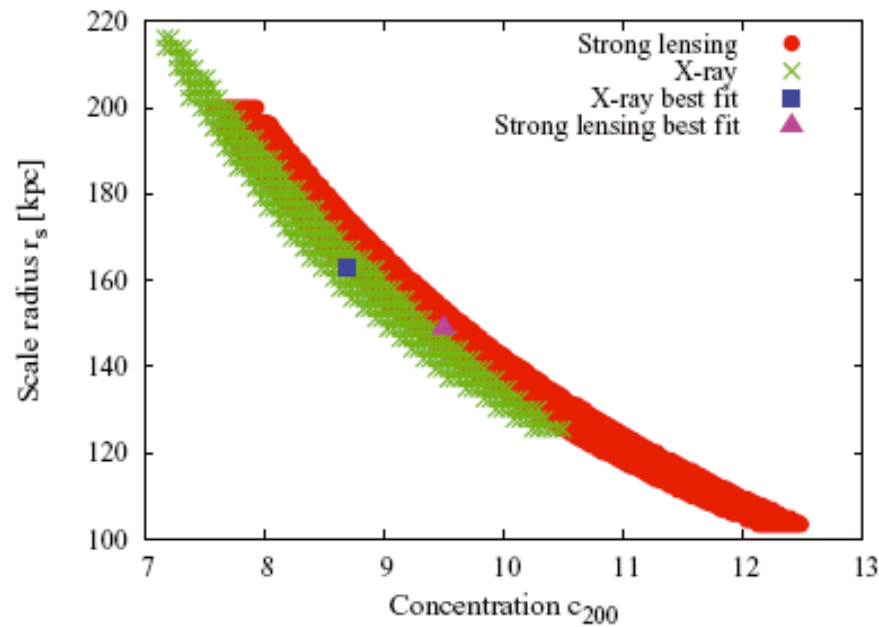


# X-ray total mass: *MS2137*



# The case of MS2137

(Donnarumma et al. 2008)



# X-ray vs Optical mass

$M_X \approx M_{\text{lensing}}$  within 15% implies

$$\frac{G M_X}{r^2} = - \frac{d(P_{\text{therm}} + P_{\text{NO-therm}})}{dr} \frac{1}{\rho_{\text{gas}}}$$

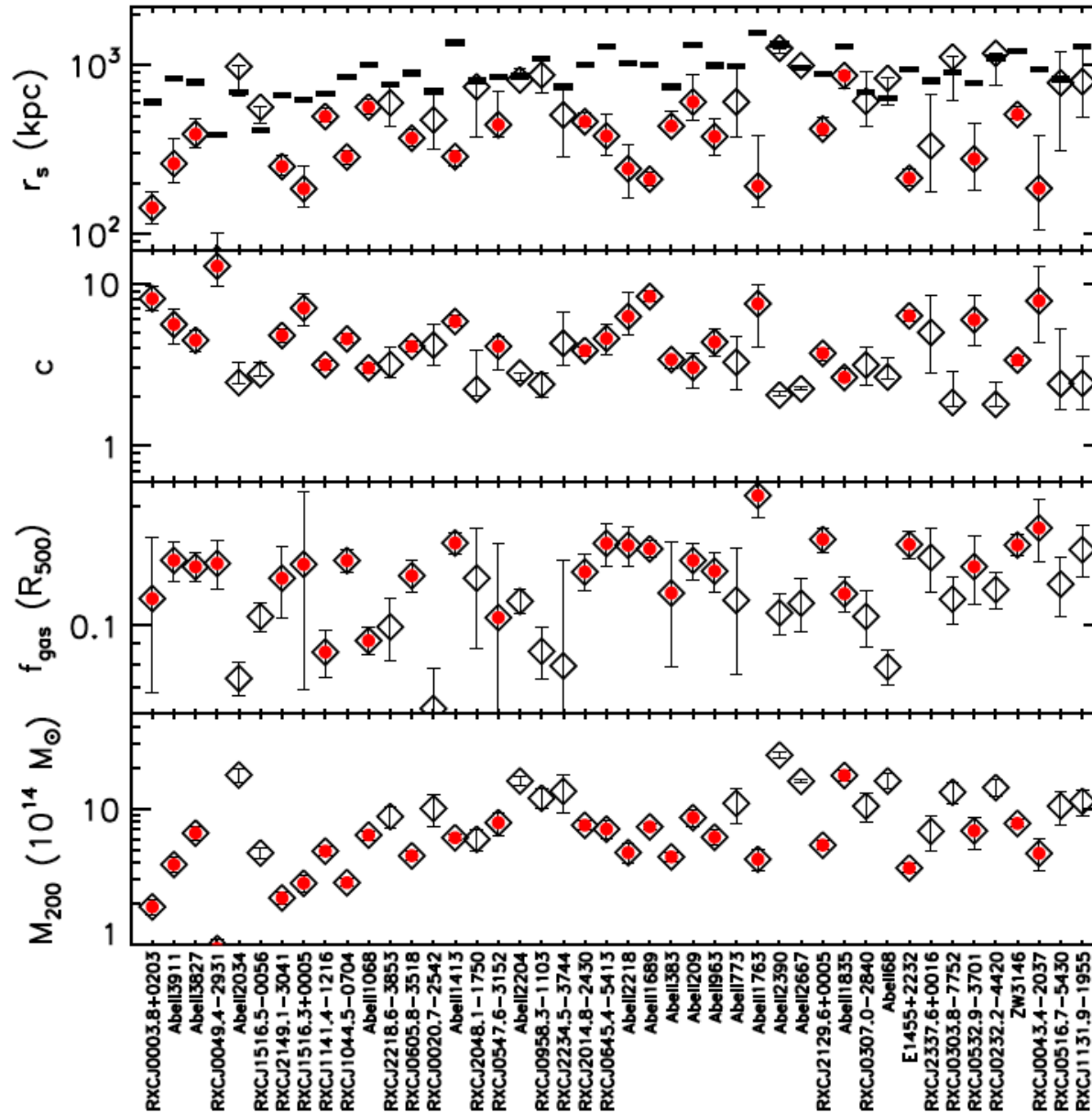
$$P_{\text{NO-therm}} \approx 0$$

Moreover, the difference btw  $M_X$  and true Mass **cannot be larger than ~20%** as proved in cosmological studies [e.g.  $f_{\text{bar}} = (M_{\text{gas}} + M_{\text{star}}) / M_{\text{tot}} = \Omega_b / \Omega_m$ ] & hydrodynamical simulations...

# Conclusions on estimate of the X-ray $M_{\text{tot}}$

- Hydrostatic equilibrium holds locally: look for relaxed regions also in merging systems
- At least two main ways (one ***forward***, one ***backward***) to apply HEE: pro/contra, no systematic is evident btw them, not thermalized ICM is missed (*but see good agreement btw X-ray/lensing data*)

# Results on $\{c, M_{\text{DM}}, f_{\text{gas}}\}$



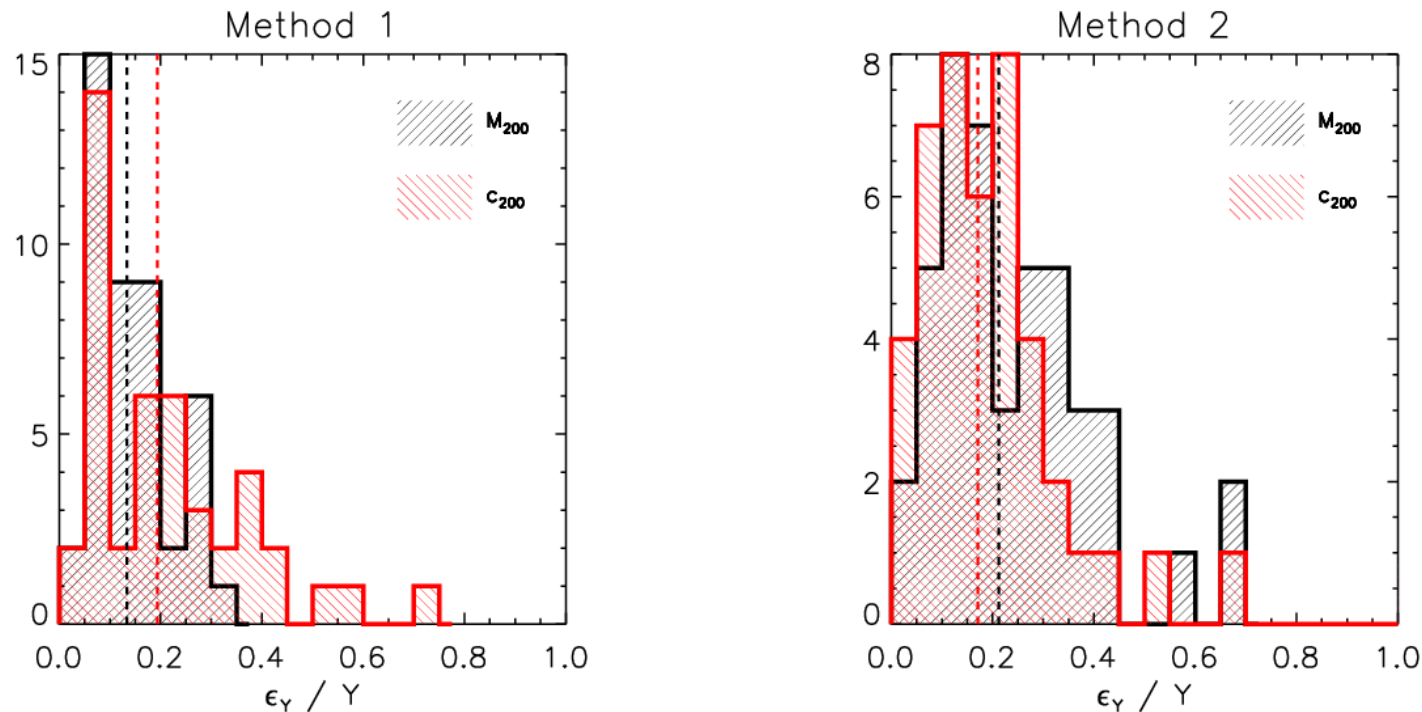
$$c = R_{200} / r_s$$

$$f_{\text{gas}} = M_{\text{gas}} / M_{\text{tot}}$$

$$M_{200} = 200 \rho_c(z) V$$

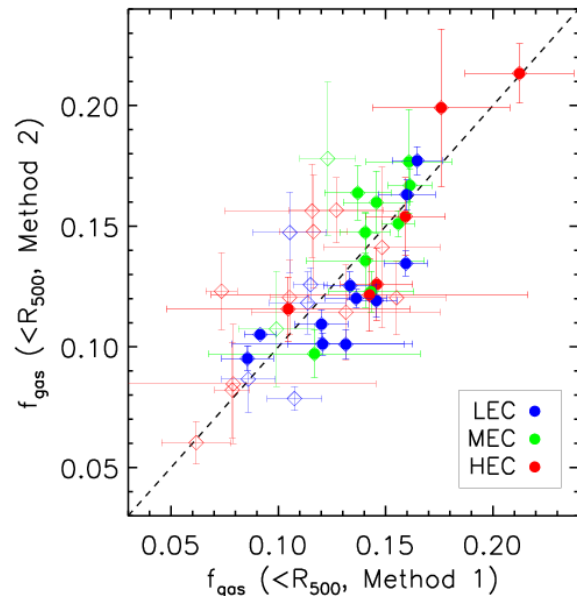
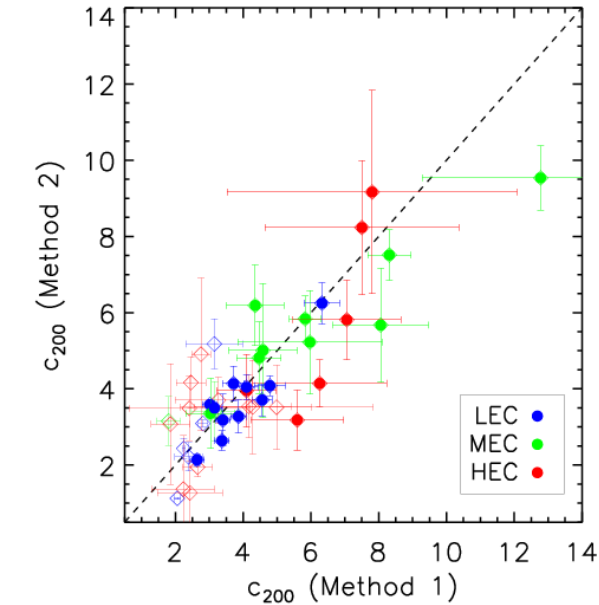
$$V = \frac{4}{3} \pi R_{200}^3$$

# The $c$ - $M_{DM}$ relation: statistical



- (*Method 1*) (de)projected data +HEE +NFW +fit  $T(r)$ :  
~15-20% relative errors on  $c_{200}$  &  $M_{200}$
- (*Method 2*) ... +functional form for  $n_{gas}(r)$  + $T_0$ :  
~20% relative errors

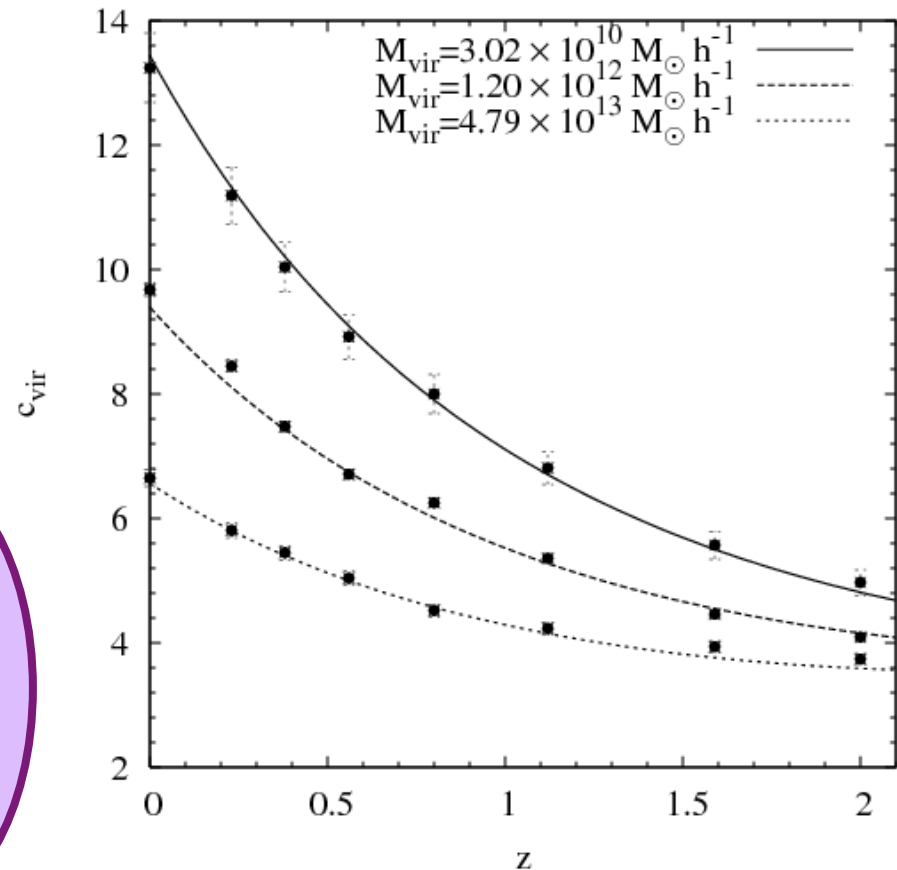
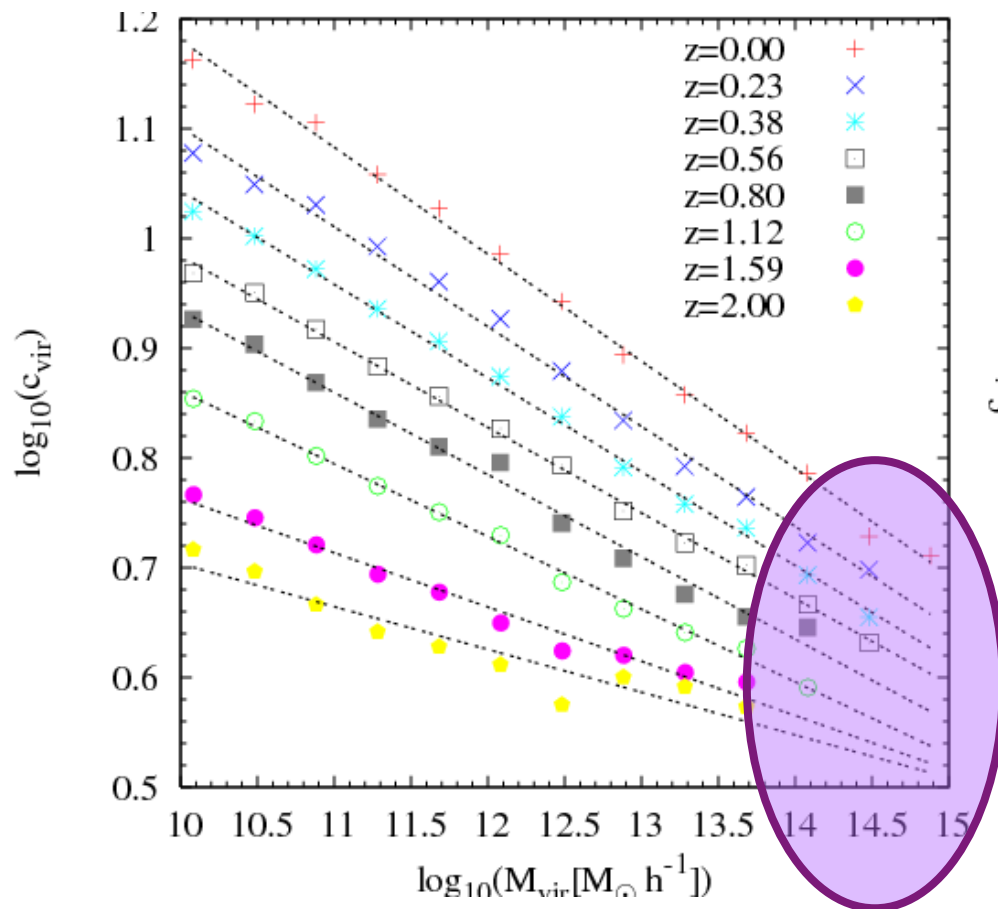
# The $c$ - $M_{\text{DM}}$ relation: systematics



Dataset	$(\hat{c}_{200} - c_{200})/c_{200}$	$(\hat{M}_{\text{DM}} - M_{\text{DM}})/M_{\text{DM}}$	$(\hat{f}_{\text{gas}} - f_{\text{gas}})/f_{\text{gas}}$
<i>Method 2</i>	-0.013	+0.008	+0.036
M2	+0.010	-0.017	+0.009
$T_{3\text{D}}$	-0.048	-0.036	+0.024
fit $n_{\text{gas}}$	+0.001	+0.011	+0.000
$P_{\text{out}}$	-0.011	+0.030	-0.014
<b>at <math>R_{200}</math></b>	<b>(-0.048, +0.010)</b>	<b>(-0.036, +0.030)</b>	<b>(-0.014, +0.036)</b>
<i>Method 2</i>	-	-0.015	+0.035
M2	-	-0.018	+0.010
$T_{3\text{D}}$	-	-0.046	+0.025
fit $n_{\text{gas}}$	-	+0.012	-0.008
$P_{\text{out}}$	-	+0.028	-0.013
<b>at <math>R_{500}</math></b>	-	<b>(-0.046, +0.028)</b>	<b>(-0.013, +0.035)</b>
<i>Method 2</i>	-	-0.073	+0.032
M2	-	-0.013	+0.008
$T_{3\text{D}}$	-	-0.059	+0.028
fit $n_{\text{gas}}$	-	+0.004	+0.000
$P_{\text{out}}$	-	+0.020	-0.009
<b>at <math>R_{2500}</math></b>	-	<b>(-0.073, +0.020)</b>	<b>(-0.009, +0.032)</b>

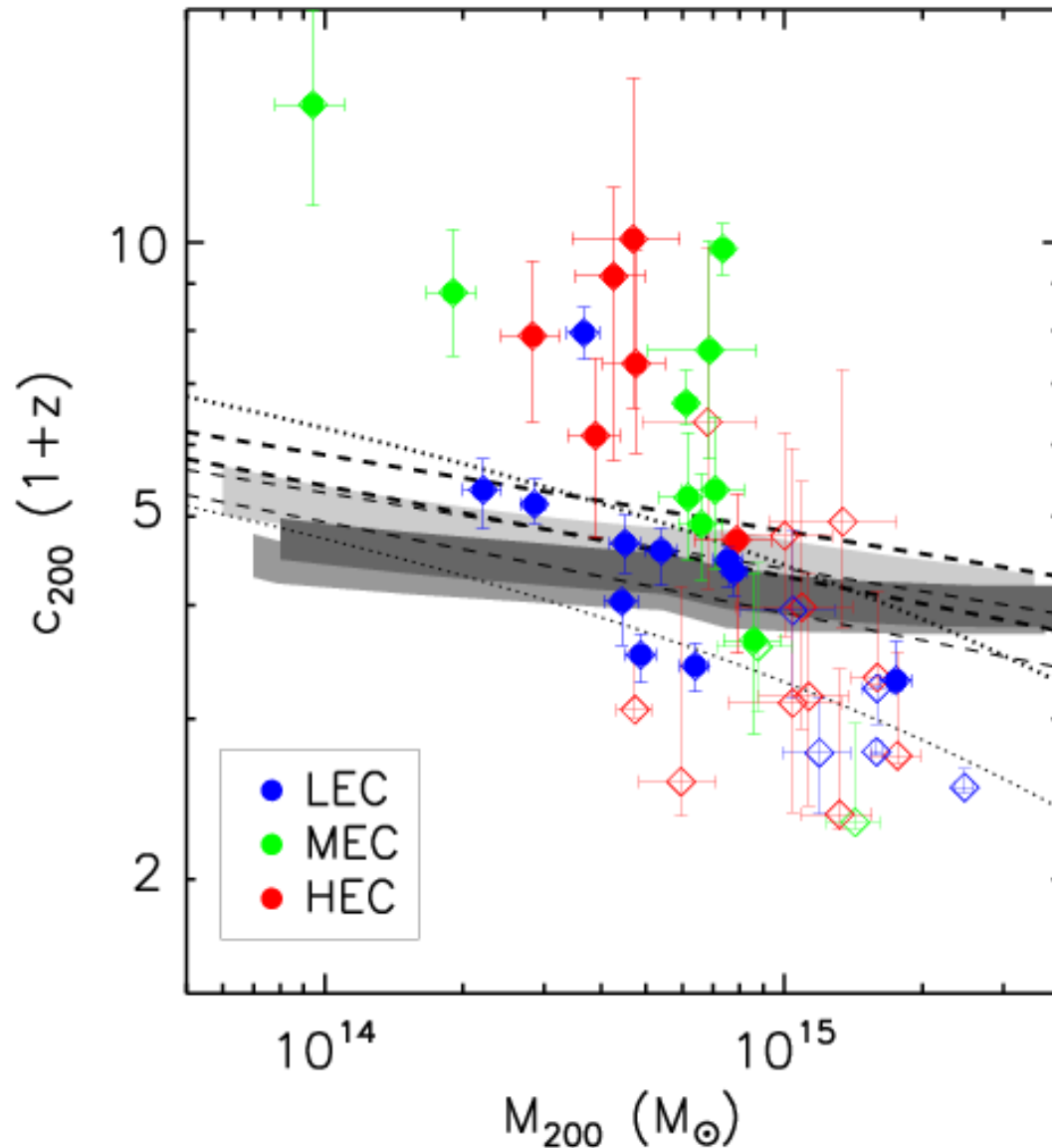
# The $c$ - $M_{\text{DM}}$ relation: $\sigma_8$ - $\Omega_m$

Concentration [ $\sim M_{200}^{1/3}/(r_s \rho_{c,z}^{1/3})$ ] depends on the halo mass growth history (function of  $\sigma_8$  &  $\rho_{c,z}$ ) and needs N-body simulations to be described as function of  $(M, z)$



(Munoz-Cuartas et al. 2010)

# The $c$ - $M_{\text{DM}}$ relation: $\sigma_8$ - $\Omega_m$



**Dotted lines:** Eke et al. (01) for a given  $\Lambda$ CDM at  $z=0$  (from top to bottom:  $\sigma_8=0.9$  and  $0.7$ ).

**Shaded regions:** Maccio' et al. (08, see Bullock et al. 01) for WMAP-1, 5 and 3 years (from the top to the bottom, respectively).

**Dashed lines** (thin:  $z=0.1$ , thick:  $z=0.3$ ) indicate the best-fit range at  $1\sigma$  in a WMAP-5 yrs cosmology from Duffy et al. (08)

Scatter in the sample

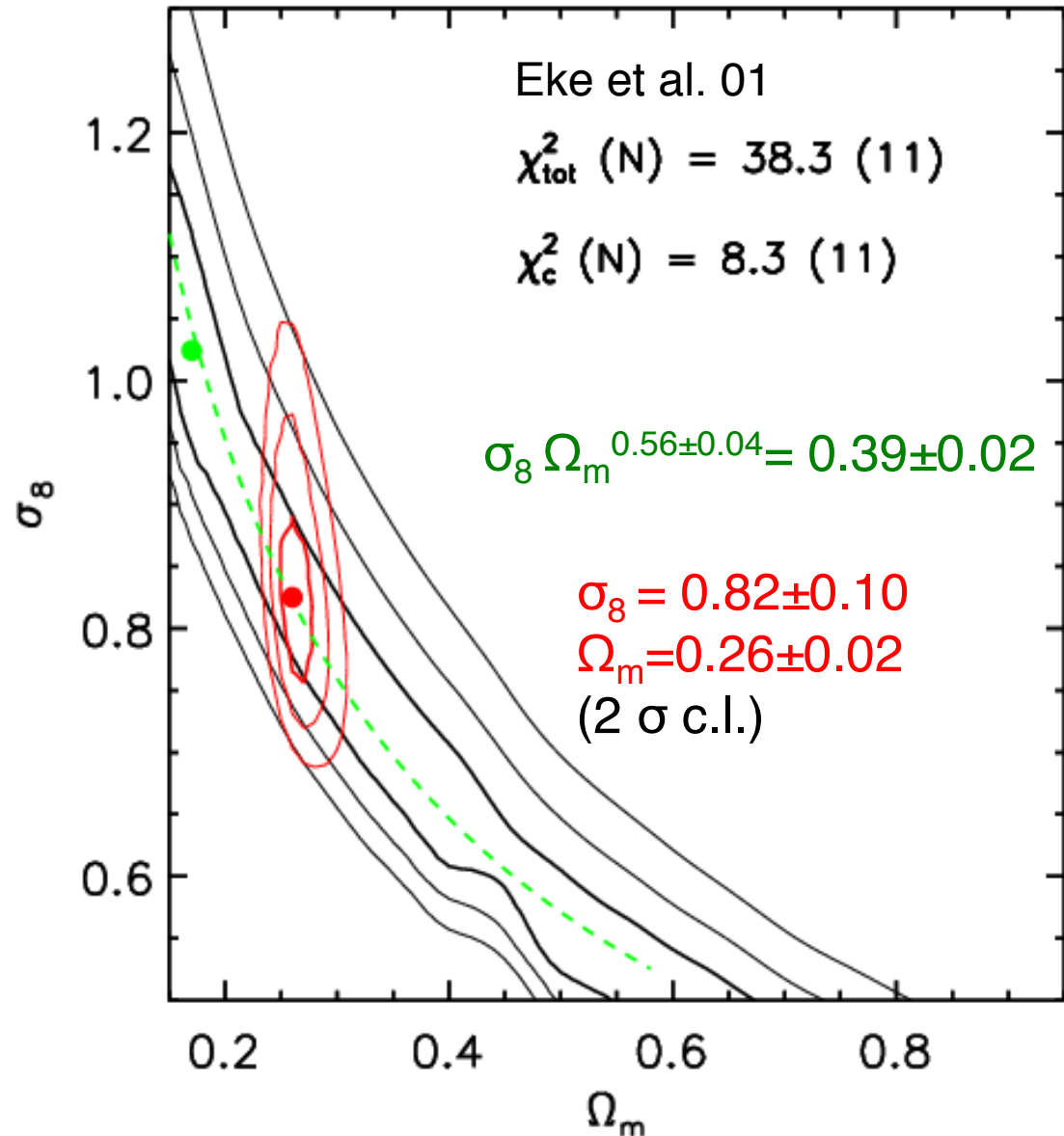
$\sigma_{\text{tot}} \sim 0.14$  ( $\sigma_{\text{stat}} \sim 0.09$ )

LEC:  $\sigma_{\text{tot}} \sim 0.08$  ( $\sigma_{\text{stat}} \sim 0.03$ )

NOTE: LEC  $\approx$  CC ... HEC  $\approx$  mergers (see e.g. Leccardi et al. 2010)

# Combining $\{c, M_{\text{DM}}, f_{\text{gas}}\}$ : $\sigma_8 - \Omega_m$

- We constrain  $(\sigma_8, \Omega_m)$  by comparing our estimates of  $(c_{200}, M_{200})$  to the predictions tuned from CDM simulations (*black contours*)
- We consider both **systematics** (e.g. different T profiles; fitted  $n_{\text{gas}}$ ; two methods:  $\sim 5\%$ ) in our measurements & **scatter** from numerical predictions ( $\sim 20\%$ , e.g. Neto et al. 07)
- We add constraints from  $f_{\text{bar}}$  (*red contours*).



# Gas mass fraction

To constrain the cosmological model

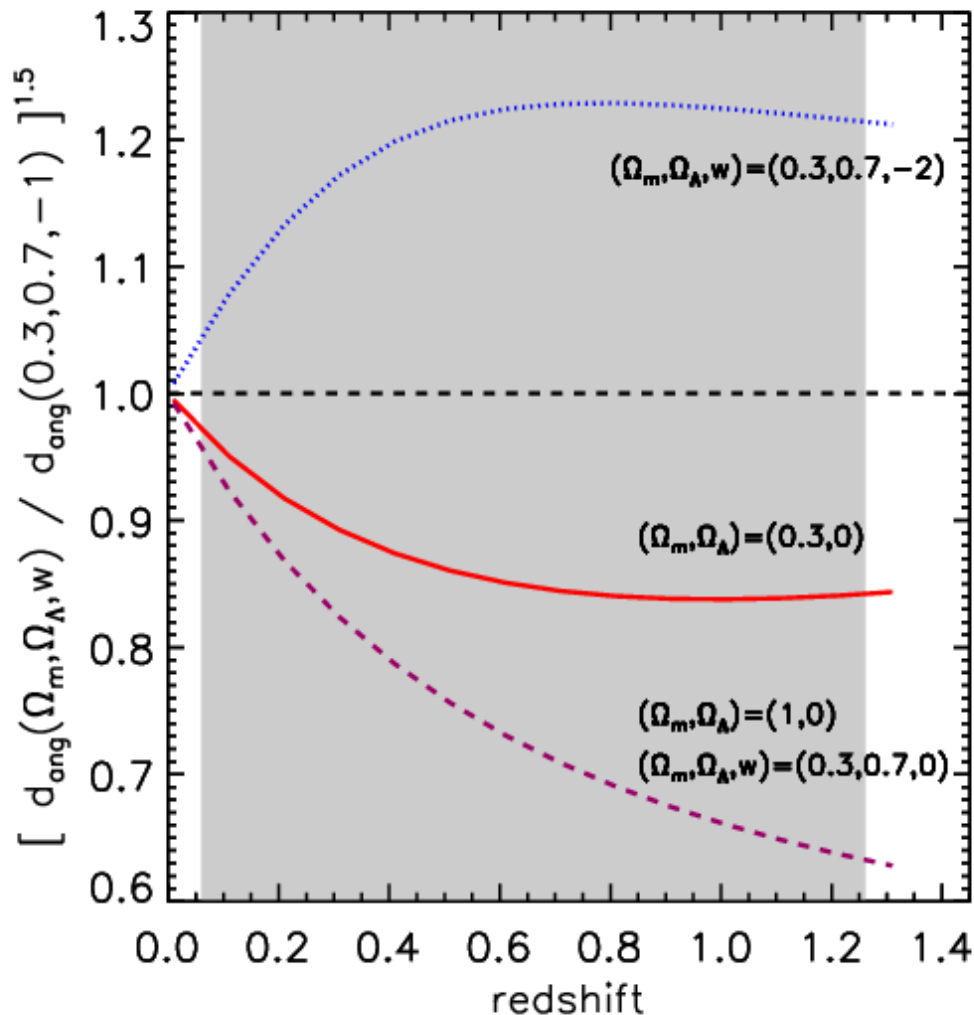
$$\Omega_m + \Omega_\Lambda + \Omega_k = 1$$

We combine a **dynamical** and a **geometrical** method  
(see also Allen et al, Blanchard et al., Ettori et al, Mohr et al) :

1. baryonic content of galaxy clusters is representative of the cosmic baryon fraction  $\Omega_b / \Omega_m$  (White et al. 93)
2.  $f_{\text{gas}}$  is assumed constant in cosmic time in very massive systems (Sasaki 96, Pen 97)

# The cosmological dependence

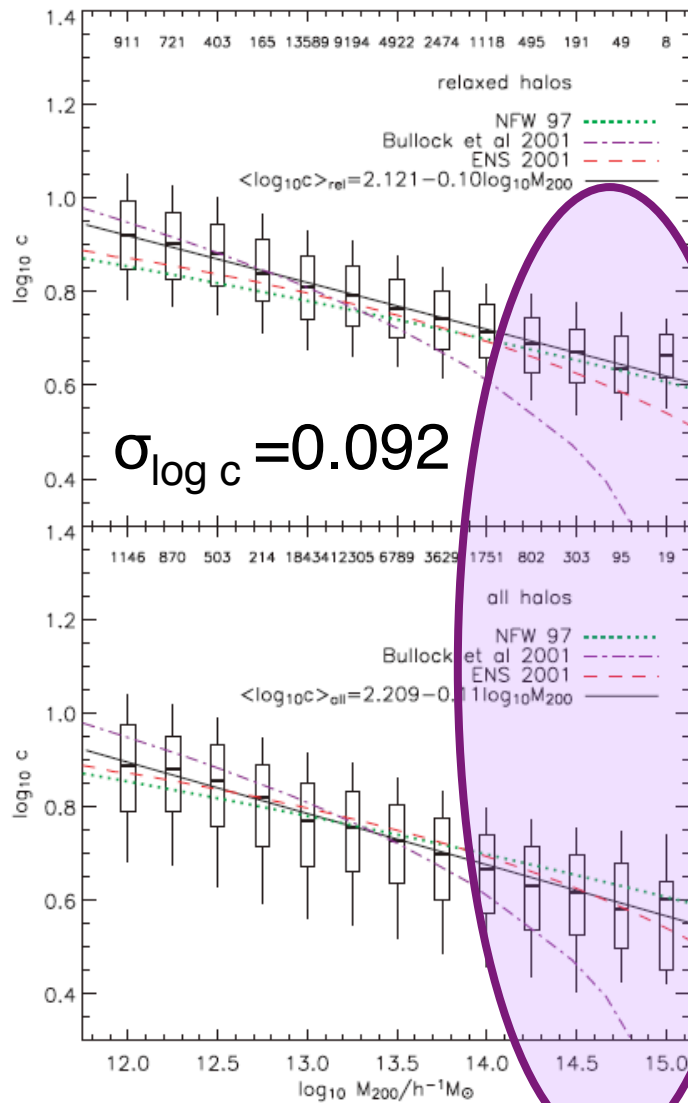
$$f_{\text{gas}}(<R_{500}) = M_{\text{gas}} / M_{\text{tot}} \propto n_{\text{gas}} R^3 / R \propto d_{\text{ang}} (\Omega_m, \Omega_\Lambda, w)^{3/2}$$



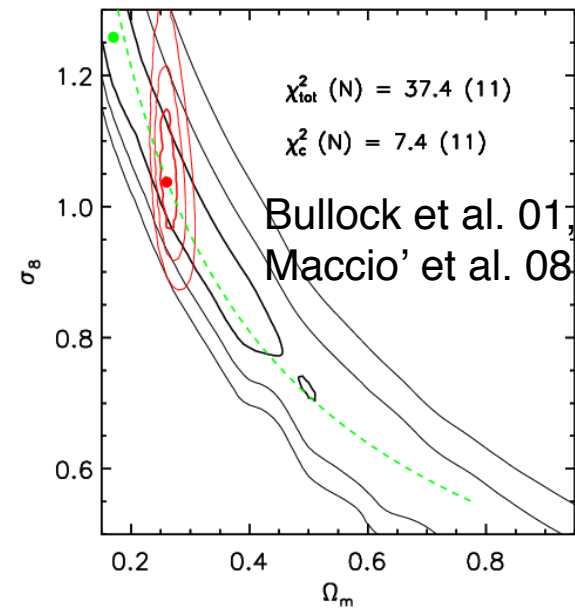
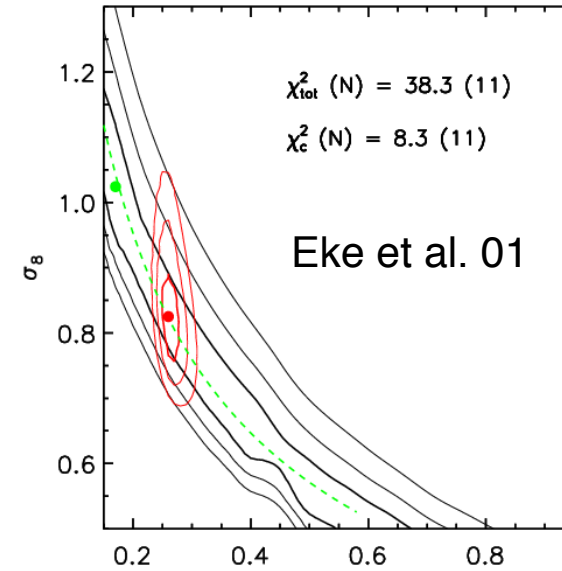
500 relaxed hot ( $T > 5$  keV) obj with  $f_{\text{gas}}$  estimate precise at 5% level provides a  $\text{FoM}_{\text{DETF}} [\sim 1/(\sigma_{w_0} \sigma_{w_a}), w = w_0 + w_a(1-a)] \sim \mathbf{15-40}$  (Rapetti et al. 08), comparable to:

- ground-based SNIa ... 8-22
- Space-based SNIa ... 19-27
- Ground-based BAO ... 5-55
- Space-based BAO ... 20-42
- Space-based clusters cts ... 6-39

# The $c$ - $M_{\text{tot}}$ relation: $\sigma_8$ - $\Omega_m$



Neto et al. 07



# Combining $\{c, M_{\text{DM}}, f_{\text{gas}}\}$ : conclusions

- We demonstrate that analysis in the  $\{c, M_{\text{DM}}, f_{\text{gas}}\}$  plane represent a mature & competitive technique to constrain  $\{\sigma_8, \Omega_m, (w)\}$
- *Our results depend ( $\sim 20\%$ ) on the models adopted to relate the properties of the DM halos to the background cosmology. A more detailed analysis of the output of larger sets of cosmological numerical simulations is requested to provide the needed calibration of massive ( $> 1e14$  Msun) DM halos as function of  $\{\sigma_8, \Omega_m, z\}$  for more definitive & robust results*

# Combining $\{c, M_{\text{DM}}, f_{\text{gas}}\}$ : conclusions

- Impact of **WDM**:

- (1) the change in core density and concentration due to the lower formation redshift in WDM models;
- (2) the suppression of density cusps due to relic thermal velocities of the WDM particles.

*Smith & Markovic* (2011) found that the former effect is the most important. Relic velocities only affect the density structure on scales  $r < 1$  kpc/h